STABILITY MEASUREMENTS IN A LOW REYNOLDS NUMBER SUPERSONIC JET

By

GERALD LEE MORRISON

Bachelor of Science

Oklahoma State University

Stillwater, Oklahoma

1973

Submitted to the Faculty of the Graduate College
of the Oklahoma State University
in partial fulfillment of the requirements
for the Degree of
MASTER OF SCIENCE
May, 1974

STABILITY MEASUREMENTS IN A LOW REYNOLDS

NUMBER SUPERSONIC JET

Thesis Approved:

D K McLaughlin
Thesis Adviser

W. A. Iiederman

Ladislaus J Fila

D P Dustan
Dean of the Graduate College

ACKNOWLEDGMENTS

The author wishes to express his appreciation to his major adviser, Dr. Dennis K. McLaughlin, and to his other committee members, Dr. W. G. Tiederman and Professor L. J. Fila, for their advice and guidance concerning this work. Appreciation is also expressed to Mr. T. R. Troutt, a fellow graduate student working on this project.

The author would like to recognize the financial support of the National Science Foundation, whose grant number GK-32686 made this study possible.

TABLE OF CONTENTS

LIST OF TABLES

LIST OF FIGURES

Figure Page

NOMENCLATURE

C	wave speed in the x direction
D	nozzle exit diameter
d	nozzle exit diameter minus twice the displacement thickness
f	frequency
k	complex wave number
k_I	imaginary part of the complex wave number
k_R	real part of the complex wave number
m	mass flux, ρu
M	Mach number
P_c	test chamber pressure (nozzle back pressure)
P_n	static nozzle exit pressure
P_o	stagnation pressure
P_p	pitot probe pressure
P_s	static probe pressure
r	radial distance from the centerline of the jet
Re	Reynolds number of jet, $\rho UD/\mu$
Re_o	Reynolds number of the hot-wire $\rho u\delta/\mu$
St	Strouhal number, fd/U
T_{rw}	recovery temperature of the hot-wire
T_o	stagnation temperature
U	mean jet velocity

u	local jet velocity
x	distance down the centerline of the jet from the exit
y	radial distance from centerline of jet in the plane of $\xi = 0°,180°$
δ	diameter of the wire
θ	Mach angle
λ_x	wavelength in the x direction
μ	viscosity
μ_o	viscosity evaluated at T_o
ρ	density
ϕ	relative phase between exciter signal and hot-wire signal
ξ	angle around azmuth of the jet
$()'$	fluctuating quantity
$(\bar{})$	mean quantity
$()_{rms}$	root mean square of a fluctuating quantity

CHAPTER I

INTRODUCTION

The mathematical representation of the noise producing mechanisms has been the major obstacle to the development of a complete jet noise analysis. Lighthill's (1, 2) classical analysis utilizes distributions of quadrupoles to represent the flow distrubances in a subsonic jet. The quadrupole source strength density is equal to a turbulence stress tensor T_{ij}, which in most flows cannot be calculated but must be estimated. Lighthill's formulation was later extended to transonic and supersonic flow (for example, see Ffowcs Williams (3)).

A new approach to the representation of the disturbances producing the sound in a jet has been an instability approach. Crow and Champagne (4) have observed latent orderly structure in a subsonic jet whose characterization can be aided with the help of the instability properties of the jet. It has been suggested by Bishop, et al. (5) among others that the noise generating fluctuations in a supersonic jet may be even more organized than in the subsonic case. They are led to this conclusion upon viewing Schlieren and shadowgraphs which show distinct wavefronts that propagate in a similar manner to Mach waves. Phillips (6) and Ffowcs Williams (3) advocate that eddies moving supersonically produce these Mach waves. However, this has not been proven adequately since few definitive measurements have been made in a supersonic jet to determine the noise producing structure of the jet.

Tam (7,8,9), Sedel'nikov (10), and Chan and Westley (11) have developed analyses which represent the noise producing disturbances in the supersonic jet in terms of linear stability theory. These theories predict values for the growth rate and wavelength of a disturbance in the jet given the frequency of the disturbance. Tam's analysis proceeds further to select the frequency of the dominant disturbance present in the jet. This selection is done by a complicated interaction between the instability waves and the cell structure of mean expansion and compression waves in the jet. Figure 1 shows the general characteristics of a supersonic jet including the mean flow cell structure. Tam, in particular, is applying a linear stability theory to high Reynolds number jets under the assumption that some orderly structure from the transition from laminar to turbulent flow will still be present in the jet.

The major direction of this research was to determine if the initial instability process in a supersonic jet can be characterized by a linear stability theory. Since a linear stability theory is most applicable for flow disturbances in a jet that is undergoing transition from laminar to turbulent flow, the jet in these experiments was run at low Reynolds numbers to stretch out the transition zone. To obtain these low Reynolds numbers, jets with exit diameters around 10 mm were exhausted into a chamber whose pressure was 1/30 of an atmosphere or less. The Mach numbers of the jets were around 2.2. To determine if a linear stability theory can be applied to the jet, the orientation, wavelength, frequency, wave speed and growth of the disturbance in the jet must be measured. Linear stability analysis assumes a solution for the flow disturbance in the form

$$u(x, r, \xi, t) = u^*(r) \exp i\,(kx-wt-n\xi)$$

for axisymmetric flow. To perform a complete stability analysis, measurements of the interdependance of the eigen values k and w corresponding to each azmuthal mode number n and the eigen function u*(r) for each n, k, and w combination should be made. Since Tam (7), Sedel'nikov (10), and Chan and Westley (11) evaluate their theories in terms of spatially growing waves, this research will do the same. Therefore, the frequency, w, and the azmuthal mode number, n, are specified to be real numbers and k is complex such that $k = k_R + ik_I$ where k_R is the wave number in the x direction and $-k_I$ is the amplification factor for exponential growth.

In view of the above discussion the following objectives were determined for this study:

1. To measure the mean flow properties of a low Reynolds number supersonic jet such as cell structure strength and profiles of the mean flow.

2. To determine if the disturbances in a low Reynolds number supersonic jet can be characterized by a linear stability theory. For the disturbances to be characterized by a linear stability theory their initial fluctuation levels must be small compared to the local mean and the disturbance must grow exponentially.

3. To determine the spectral content of the fluctuations present in the jet.

4. To measure the wavelength and wave speed of some of the dominant spectral components.

Calculations of Sedel'nikov (10) were performed for a hot jet while Chan and Westley's (11) were for a helium jet. Therefore, their published results are not applicable to the cold jets used in this study.

However, Tam's analysis (7) was performed for a cold jet and will, therefore, be compared to the measurements made in this study.

CHAPTER II

EXPERIMENTAL APPARATUS AND PROCEDURE

The experiments were performed in the Oklahoma State University free jet test facility. This test facility utilizes three axisymmetric supersonic de Laval nozzles with a design Mach number of 2.65 for invisid flow. The exit diameter of the three nozzles are 6.35, 9.52 and 15.9 mm. The two smaller nozzles have conical contours with half angles of 1.60° and 2.28° for the 6.35 mm and 9.52 mm nozzles respectively. The 15.9 mm nozzle has contoured walls designed by the method of characteristics for uniform parallel flow at the exit. Two millimeters upstream of the exit of a nozzle is located a static pressure tap for measuring the nozzle exit pressure.

The jet exits into a chamber that is lined with 1.5 cm thick acoustic tile as illustrated in Figure 2. The purpose of this acoustic tile is to reduce the amplitude of the reflected sound waves. The pressure in the chamber is controlled by a variable area diffuser and maintained very close to the nozzle exit pressure (around 0.5 cm of mercury). The diffuser exits into a 31.8 cubic meter vacuum storage tank which is evacuated by a Kinney vacuum pump. The tank serves effectively to damp out disturbances that might propagate upstream from the vacuum pump and also enables short duration experiments with large nozzles.

The inlet of the supersonic jet consists of a stilling chamber that is vented to atmosphere by a valve which controls the jet stagnation

pressure. There is a five centimeter thick section of foam rubber followed by six fine screens in the stilling chamber. In this manner a flow that is relatively free of disturbances is produced. The cross sectional area of the 15 cm diameter stilling chamber is in all cases more than 150 times larger than the nozzle exit area.

The test chamber is equipped with a two degree of freedom probe drive on which hot-wire, pitot pressure, static pressure and microphone probes are mounted. The drive traverses the jet in the x and r directions passing through the centerline of the jet.

Pressure probes were connected to either a silicone oil (specific gravity of 0.93) or a mercury manometer, both of which were referenced to a vacuum of 30 microns of mercury. If the pressure measured was less than 3.5 cm of mercury the silicone oil manometer was used for better resolution. The pitot probe is a square ended tube epoxied onto a brass wedge. In supersonic flow the pitot probe measures the stagnation pressure behind a normal shock. Matthews (12) calibrated this type of probe and at the Reynolds number range of this study the viscous correction was negligible. The static pressure probe was a slender cone probe with a diameter of 0.88 mm and is shown in Figure 3 along with the pitot probe. From Behrens' (13) calibration of a probe of this design, it was determined that the viscous correction is negligible for this application. Knowing the stagnation pressure behind a normal shock and the static pressure, one is able to calculate the Mach number at the location of the measurement. The Mach numbers presented in this paper were determined in this way.

Disa 55A53 subminiature hot-wire probes epoxied to brass wedges similar to the pressure probe wedges were used in this study. A Disa

model 55D01 constant temperature anemometer was used to operate the probes in conjunction with Disa D.C. (55D30) and RMS (55D35) voltmeters and an auxilliary unit (55D25) which contained a frequency band pass. Frequently a Multimetrics model AF 120 active filter was used to band-pass the signals.

Profiles of mean hot-wire voltage were made by driving the probe across the jet with the radial probe drive which was coupled to a potentiometer to provide a D.C. voltage proportional to the position of the probe. This voltage was input into the y axis of a Moseley 2D x-y recorder and the mean bridge voltage was input into the x axis. In this manner, the profile of the mean hot-wire voltage signal was obtained at several x/D locations. The same technique was used to obtain profiles of the hot-wire voltage fluctuations using a Ballentine AC to DC converter to convert the fluctuating hot-wire voltage to a DC voltage.

An extensive calibration procedure is required to decompose the hot-wire voltage fluctuations into temperature, velocity and density fluctuations as shown by Morkovin (14). When measurements are performed in a continuum flow ($Re_o > 20$) a data reduction scheme such as the one presented by Rose (15) may be used. According to Behrens (16) the flow around the hot-wire probe is in a transition from continuum to non-continuum flow for Re_o between 20 and 0.2. In this region the recovery factor (T_{rw}/T_o) is not constant. When coupled with the large end loss correction, the decomposition of the hot-wire signal is further complicated. Behrens (17) has suggested a reasonable accurate simplification which will be incorporated in this study. For large overheat ratios, e'/E equals $(A_m)\ m'/\bar{m}$. By calibrating the hot-wire probe over the range of mass flux in which it is to be operated, the factor (A_m), which is

the local sensitivity of the curve of mass flux versus hot-wire mean voltage, can be determined.

Characterization of the orientation, wavelength, and wave speed of spectral components of the instability requires phase measurements. The technique chosen in this investigation consists of artificially exciting the instability and using the excitation signal for a reference from which to make phase measurements. In the two smaller nozzles a tungsten electrode was mounted on the wall opposite the pressure tap two millimeters from the exit. The electrode was used to excite the jet artificially with an oscillating glow discharge in a manner similar to the technique used by Kendall (18). The glow discharge is produced by applying a 800 volt peak to peak alternating voltage biased to a negative potential of 450 volts. In this manner an oscillating glow is established.

To determine if the glow discharge had any effect on the hot-wire signal, such as residual heat being convected downstream by the jet, the electrode was mounted directly upstream of the hot-wire probe so that the flow passing through the glow also passed over the hot-wire probe. The electrode was then mounted on the opposite side of the jet. It was determined that the glow had no appreciable effect on the hot-wire signal. This would be expected since the total energy flux of the jet is 100 times larger than the energy flux introduced into the flow by the glow discharge apparatus.

Phase shift between the glow exciter input signal and the hot-wire voltage fluctuations were evaluated from oscilloscope traces of the two signals for several x/D locations to determine the wavelength of the distrubance in the x direction.

Frequency spectra of hot-wire voltage fluctuations were obtained using a Hewlet Packard model 302A wave analyzer with a constant band width of 6 Hertz and a sweep rate of 1000 Hertz per minute. The spectra from the 302A wave analyzer were compared with the spectra from a General Radio model 1910A wave analyzer with a constant band width of 100 Hertz. The output from the wave analyzer was recorded on a Moseley 2D x-y recorder. Frequently data was recorded on either a Sanborn 2000 or an Ampex FR 1300 tape recorder, both with frequency response well above 60,000 Hertz. A General Radio 1523-P4 wave analyzer was used in the 100 Hertz bandwidth mode to band pass hot-wire voltage fluctuation signals in order to determine the change in amplitude of the fluctuations about one frequency as the probe is progressed downstream. In this manner the growth of the disturbance at that frequency can be determined.

CHAPTER III

EXPERIMENTAL RESULTS

Mean Flow Measurements

Pitot pressure and static pressure measurements were made along the centerline of the 6.35 and 9.52 mm jets. It was found that even when the nozzle exit pressure was approximately the same as the chamber pressure (P_n/P_c = 1.01) there was a cell structure of expansion and compression waves present. Figure 4 illustrates how the static and pitot pressure measurements vary along the axis of the 6.35 mm jet at a Reynolds number of 12,100. Assuming isentropic flow down the centerline of the jet it is possible to calculate a local Mach number of the jet from each of the three ratios P_p/P_o, P_s/P_o and P_s/P_p. The variations in pitot pressure measurements (P_p/P_o) indicate a larger variation in Mach number as one moves downstream than the variations in static pressure measurements (P_s/P_o) do. This may be explained by the fact that the static probe is long and effects the flow before the flow reaches the measuring orifices on the probe. It is therefore possible that the static probe tends to smooth the flow thus decreasing the magnitude of the variations in the static pressure measurements slightly.

It has been determined that the stagnation pressure decreases as the air flows through the nozzle. Therefore, one must evaluate the local Mach number from the local measurement of P_s and P_p. When one takes into

account the smoothing effect of the static pressure probe and combines the static and pitot pressure measurements (P_s/P_p) it can be determined that the Mach number varies $\pm$ 3.5% on the centerline of the jet. This corresponds to a $\pm$ 6% variation in mass flux along the centerline of the jet.

It was observed that the ratio P_n/P_o changed slightly from day to day with corresponding change in Mach number. This variation seems to be caused by changes in the amount of moisture in the air. Days with more moisture in the air yield higher values of P_n/P_o, and hence indicate a lower Mach number. Better measurement and control of the humidity in the flow facility is needed to fully determine the effect of humidity upon the ratio of P_n/P_o.

The data in Figure 4 was used in conjunction with other measurements of the same type to determine an average Mach number of 2.2 for the 6.35 mm jet. An average Mach number for the 9.52 mm jet was calculated to be 2.3. From hot-wire measurements it was estimated that the Mach number for the 15.9 mm jet was 2.5. The difference in Mach number from the design Mach number of 2.65 is attributed to viscous effects in the nozzles since the area ratio in all three nozzles is 3.036.

Mean hot-wire measurements were made along the centerline to determine the magnitude of the cell structure in the 6.35 mm and 9.25 mm jets at different pressure balance conditions. Figure 5 parts (a) and (b) show mean hot-wire voltage measurements in the 6.35 mm jet when the ratio of the nozzle exit pressure to the chamber pressure is 1.01 and 1.5. As to be expected, the cell structure of compression and expansion waves is stronger when the pressure ratio is 1.5. The arbitrary linear scales presented are the same in all three parts of Figure 5. Part (c) of the

figure presents mean hot-wire voltage measurements along the centerline of the 9.52 mm jet operating in the perfectly balanced condition (P_n/P_c = 1.01). The data was taken with the same hot-wire probe operating at the same overheat ratio as in parts (a) and (b). The cell structure in the 9.52 mm perfectly expanded jet is much stronger than in the 6.35 mm perfectly expanded jet. This may be due to the larger divergence angle of the 9.52 mm nozzle. The cell length of the two jets in the perfectly expanded condition are both approximately equal to 2.0 D. When underexpanded the cell length elongates to 2.5 D. Figure 6 illustrates the elongation process in the 9.52 mm jet. The cells elongate in a continuous fashion with no apparent discontinuities as the pressure ratio P_n/P_c is increased.

Mean hot-wire voltage profiles are presented in Figure 7 at various x/D locations for the 6.35 mm and 9.52 mm jets. These were included to demonstrate that the profiles can be approximated by top hat profiles for at least the first four diameters of flow. The top hat profile was used in the development of the instability theories mentioned earlier.

Frequency Spectra

Figure 8 presents representative hot-wire voltage fluctuation frequency spectra for the three nozzles used in this study operating in the perfectly expanded condition. The frequency is nondimensionalized by U/d to yield a Strouhal number where U is the mean velocity of the jet and d is the effective diameter. The effective diameter is the diameter of the nozzle minus twice the displacement thickness of the boundary layer. The hot-wire probe is located five diameters downstream of the exit in the bottom shear layer at the point of maximum fluctuations.

Since there is a major mode in all three frequency spectra at a Strouhal number of St ≃ 0.18, we must conclude that this frequency is characteristic of the supersonic jet flow. The 15.9 mm jet also has two modes present at Strouhal numbers of 0.27 and 0.28. The exact reason for the modes at higher Strouhal numbers is not known at the present time. The spectras in the smaller nozzles all drop off drastically in magnitude above a Strouhal number of 0.20 but sometimes contain a minor peak at a Strouhal number of 0.36 (twice the frequency of the donimant mode). This decrease in magnitude is not due to the lack of hot-wire frequency response.

After recording over 50 spectra at various locations in the jet for various mean flow conditions, it has been determined that very few are exactly the same. However, virtually all of the spectra of the 6.35 mm jet have recurring dominant modes at St = 0.148, 0.176 and 0.185. In numerous cases (but not all) the 9.52 mm jet has only one dominant mode at St = 0.17 provided that the probe is upstream of x/D = 5. It has also been observed that the exact characteristics of a frequency spectrum depend upon the pressure balance condition and on the humidity of the air.

Figure 9 illustrates the effect of increasing the Reynolds number on the hot-wire spectra of the 9.52 mm jet. All spectra were taken at x/D = 5 at the point of maximum fluctuation. The dominant oscillation remains present but other frequencies increase in amplitude compared to the peak spectral component as the Reynolds number is increased. The Strouhal number of the peak decreases slightly as the Reynolds number is increased.

Hot-Wire Fluctuation Amplitude Measurements

Profiles of hot-wire voltage fluctuations are shown in Figure 10 for the 9.52 mm naturally excited jet. Note that the potential core (area of negligible fluctuations in the center of the jet) lasts for only about 6 diameters for this Reynolds number range. Hot-wire voltage fluctuation measurements made at the point of maximum fluctuations on the bottom shear layer of the 6.35 mm jet are shown in Figure 11 for various x/D locations. The values for $m'_{rms}/\bar{m}$ were obtained utilizing the hot-wire calibration technique described before in this paper

$$m'_{rms}/\bar{m} = \frac{1}{A_m} e'_{rms}/E.$$

The sensitivity coefficient A_m was determined by direct calibration in mean flow measurements.

It was observed that near the exit of the nozzle a majority of the fluctuations were caused by low frequency disturbances (St < 0.01). These low frequencies are enhanced by the resonance of the test chamber and, therefore, do not give a true representation of a free field jet. When the same data was reduced using 1 KHz high pass filter to eliminate the low frequency components, the axial distributions of mass flux fluctuations in Figure 12 were obtained. The per cent fluctuations at x/D = 1 are less than four per cent of the local mean.

In order to obtain growth rates for a single spectral component, the hot-wire signal was bandpassed about the frequency to be observed with a 100 Hertz wide bandpass. This technique was utilized for the frequencies of 15.4, 18.2 and 19.1 KHz, which correspond to major peaks in the naturally occurring spectra. The resulting graphs for $m'_{rms}/\bar{m}$ versus x/D are shown in Figure 13. These measurements were performed at

the radial location of maximum fluctuation for the entire spectrum of disturbances present. This position may not coincide with the position of maximum fluctuation for a given spectral component. Therefore, the growth rates derived from them are only a preliminary indication of how the disturbances grow.

Using the linear stability theory assumed solution form for the mass flux fluctuation

$$m' = \text{Real}\,(m(r)\exp i\,(kx - wt - n\xi))$$

one is able to determine that

$$-k_I d = \frac{d(\ln(m'/\bar{m}))}{d(x/d)} .$$

From this equation and the data in Figure 13 one is able to determine the amplification factor, $-k_I d$, for the region of exponential growth. The disturbances grow exponentially for about five diameters where the spectral component reaches approximately 5% of the local mean. Here non-linear effects begin to dominate the flow.

The mass flux fluctuation data plotted in Figure 13 are for the 6.35 mm jet at a Reynolds number of 28,900. Similar measurements were made at Re = 9,600 and Re = 19,300, and the growth rates were all within 30% of each other with no systematic Reynolds number dependence evidenced. However, measurements indicate that for a Reynolds number of 3,600 the instabilities in the 6.35 mm jet did not grow and the jet remained completely laminar for at least ten diameters.

Comparison of numerical values of growth rates at Re = 28,900 with theoretical predictions are shown in Table I. Recalling from Figure 13 that the St = 0.148 mode has the largest amplitude, it is encouraging

that Tam's theory (7) does a good job of predicting its growth rate. More measurements are needed to better explain the behavior of the other modes.

In summary it was found that the disturbances in the jet originate with small fluctuation amplitudes and grow exponentially for the first five diameters of flow. Since this is in accordance with linear stability theory, we conclude that the flow disturbances are in fact instability waves.

Wavelength and Wave Speed Measurements

The 6.35 mm jet was artifically excited at three different frequencies to determine the wavelength (and wave speed) of the disturbance at that frequency. It is, therefore, important to determine the effect of this excitation upon the naturally developing instability process in the jet. Figure 14 contains a naturally excited spectra and three artificially excited at 15.5 (St = 0.15), 19.4 (St = 0.18) and 22.3 (St = 0.21) KHz. The arbitrary linear scale is the same in all four parts of the figure. These four spectra were recorded on a humid day. The major effect of the higher humidity was that the multimodal characteristics of the naturally occurring spectra were suppressed. However, more data needs to be taken before any conclusive correlations can be drawn between the humidity and the resulting spectra. The 19.4 Khz excitation frequency corresponds to the dominant natural mode of St = 0.18. The 15.5 KHz was a major mode that was usually present in hot-wire frequency spectra. The 22.3 KHz mode was not a major mode in any spectra but was excited since it responded favorably to excitation.

It was found that it was possible to excite the jet with the glow discharge at many different frequencies. As one swept through the frequencies there would intermittantly be instabilities that would respond by phase locking onto the exciter. When the 19.4 KHz mode was excited, spectra like the one in Figure 14(b) were obtained in all cases no matter what the humidity was. The multimodal characteristic of the jet is suppressed when excited at the dominant natural mode in all cases. However, when exciting at 22.3 KHz, the results differed somewhat. In most cases the 19.4 KHz mode was suppressed, but the rest of the spectra was the same as the naturally occurring spectra except for the added peak at 22.3 KHz.

When the jet was excited at 15.5 KHz, the spectrum in Figure 14(d) was obtained. This excitation frequency did not diminish the peak at 19.4 KHz appreciably but did add a peak at 15.5 KHz, 4 KHz and 12 KHz. The two harmonic modes, 4 and 12 KHz, no doubt relate to the work done by Miksad (19) in a subsonic free shear layer that was artificially excited at two frequencies (f_1 and f_2). He found that the instabilities produced by the excitation caused other disturbances to be present with frequencies of the form $f = (nf_2/m \pm (pf_1/q)$ where n, p = 1, 2, 3, ... and m, q = 1, 2. In this case the jet was naturally excited at 19.4 KHz and artificially excited at 15.5 KHz. The two resultant frequencies in the spectra are represented by $f_2 - f_1$ and $f_2 - \frac{1}{2}f_1$ where f_2 = 19,400 Hz and f_1 = 15,500 Hz. Sato (20) also observed this type of phenomena in a two dimensional wake. The harmonic modes appear to be due to non-linear interaction between f_1 and f_2. The reason for the 22.3 KHz excitation not resulting in the same non-linear effect is not known. The

fact that excitation at different spectral components does not result in the same non-linear interaction shows that there is still a good deal to be learned about the instability process.

The variation of phase between the glow exciter signal and the hot-wire voltage fluctuation as one progresses in the x direction was measured from oscilloscope traces like the one in Figure 15. This photograph is a 1/5 second time history of the signals with the hot-wire probe located at x/D = 5. Phase measurements were not made unless this degree of locking between the exciter and the hot-wire signal was obtained. By plotting phase angle ϕ versus x/D one is able to determine the wavelength, λ_x, in the x direction.

Values of λ_x were determined for the 9.52 mm jet by exciting the jet at its natural dominant mode (St = 0.17) and plotting the phase measurements versus x/D (Figure 16). By using a least squares linear regression analysis, it was determined that the wavelength (λ_x/D) for this data was 3.36 ± 0.15 which includes only random error uncertainty. The error band is the 95% confidence interval. λ_x varied from day to day so additional phase shift data was taken on different days and the best estimate of λ_x/D is 3.30 ± 0.3 where the uncertainty limits include random and systematic errors.

Using the 6.35 mm jet it was possible to excite the jet at many different frequencies. Figure 17 shows the phase plots for the jet being excited at (a) St = 0.18, (b) St = .21, and St = 0.15. Presented in (a) is data from three different days. The absissa intercept changes from day to day. It is possible that this is due to the manner in which the glow exciter electrode erodes with time changing the geometric configuration of the glow and thus altering the phase of the instability

wave at the exciter. A complicated interaction with the moisture in the air is also a possible cause for the changing intercept. We believe the changing humidity to be the cause of the wavelength changing from day to day. Using the least squares linear regression analysis, it was found that the following wavelengths (λ_x/D) are present in Figure 17(a): 3.18 ± 0.18, 3.34 ± 0.16, 3.03 ± 0.12, where the error is the 95% confidence interval for each measurement. The best estimate of the average wavelength (λ_x/D) is 3.2 ± 0.3.

Part (b) of the figure is a phase plot when the 6.35 mm jet was excited at St = 0.21. The wavelength in this case was determined to be 2.57 ± 0.18. In Part (b) the jet was also excited at St = 0.15 and this wavelength was determined to be 3.88 ± 0.16. The wavelengths in part (b) also varied day to day so best estimates of the wavelengths (λ_x/D) average are 3.8 ± 0.30 and 2.55 ± 0.25 for St = 0.15 and St = 0.21 respectively. When one computes the wave speed of the disturbance in the x direction ($C = \lambda_x f$) for all three modes, it was found that they are equal within the accuracy of the measurements (10%). The wave speeds were as follows: St = 0.15, C = 0.70U; St = 0.18, C = 0.73U and St = 0.21, C = 0.68U. Therefore, over the range of excitation that was used in this study, it is evident that the waves travel downstream in the jet at the same convection speed regardless of their frequency, within the accuracy of the measurements.

The change in λ_x (Figure 17(a)) does not seem to be a Reynolds number effect since the Reynolds number was essentially the same for all three days. Variation in the pressure balance P_n/P_c was eliminated since the same pressure balance was maintained on the different days. It has been observed that the wavelength seems to shorten as the humidity is

increased. This would seem reasonable since increases in humidity also seem to increase the ratio P_n/P_o. An increase in P_n/P_o indicates a decrease in Mach number, and since the disturbances seem to propagate at a given percentage of the velocity, the wavelength would shorten if excited at one given frequency (const. = C/U; const = $\lambda_x f/U$). However, this correlation does not always hold true for all measurements but is only a general trend.

Hot-wire measurements in the 6.35 mm and 9.52 mm jet indicate that the relative phase ϕ differs by 180° at a given x/D location between the upper and lower shear layer. This was observed for the St = 0.18 and St = 0.15 modes in the 6.35 mm jet and for the St = 0.17 mode in the 9.52 mm jet. Although this evidence is not conclusive, the data strongly indicates that the major modes have an n = 1 azmuthal mode dependence. This means that the wavefronts are helicies rather than axisymmetric disturbances as measured in the subsonic jet by Crow and Champagne (4).

Tam's analysis (7) has the capability to predict the real part of the wave number ($k_R = 2\pi/\lambda_x$) when the frequency of the disturbance is given. Therefore, this theory will be compared to the measured values of $k_R d$ for the three modes excited in the 6.35 mm jet and the one mode excited in the 9.52 mm jet. Table II contains all of these values along with the Strouhal number of the dominant mode predicted by Tam's analysis. The value of $k_R d$ which corresponds to the predicted dominant mode's frequency is presented in parenthesis below the Strouhal number of that mode. The comparison of $k_R d$ shows reasonably good agreement between the measurements and Tam's theoretical predictions. The analysis does not

predict the multimodal process present in the jet. However, the dominant frequency predicted by Tam's analysis is in the range of the major modes present in the jet.

CHAPTER IV

CONCLUSIONS

The mean flow properties of a supersonic axisymmetric low Reynolds number jet were measured. It was determined that the mean flow can be approximated by a top hat profile for at least the first four diameters of the flow. The disturbances in the jet can be characterized as instability waves since they grow exponentially and originate with small fluctuation amplitudes compared to the local mean. This is in accordance with linear stability theory.

The measured growth rates for the largest amplitude dominant mode was in good agreement with the predicted value of Tam. Little Reynolds number dependence in the growth rate was observed except that below Re = 3,600 the jet remained completely laminar for over ten diameters.

From hot-wire frequency spectra it was concluded that in the 9.52 mm jet there is a major mode present whose Strouhal number is 0.17. In the 6.35 mm jet, which is multimodal, there were recurrent major spectral components present at St = 0.148, 0.176 and 0.185. Thus, In general, Tam's single frequency selection mechanism is not verified by experiment. However, the predicted single frequency does fall among the several frequencies measured in the 6.35 mm jet.

The wavelengths of some of the dominant spectral components were measured. The wave speed calculated from them indicates that these disturbances were all propagating down the jet at about 70% of the mean jet

velocity. The wavelengths predicted by Tam agree favorably with the measured values.

CHAPTER V

OBSERVATIONS AND RECOMMENDATIONS FOR FUTURE WORK

This section will present some aspects of the research that were not presented earlier since they did not directly apply to the major objectives of the thesis and some of the measurements are preliminary in nature. The multimodal characteristics of the 6.35 mm jet was the major question left unsolved in the thesis. In an effort to determine the reason for the 6.35 mm jet being single modal the following measurements were made.

All frequency spectra presented until now in the thesis have been for the perfectly expanded jet. Hot-wire spectra of the 6.35 and 9.52 mm jets operating in both perfectly expanded and underexpanded conditions (P_n/P_c = 1.5) are presented in Figure 18. In the underexpanded case the multimodal feature of the 6.35 mm jet has diminished in that there are less major modes, the modes present are grouped closer together and at a lower range of frequencies. In Figures 5 and 6 it was seen that in the underexpanded condition the strength of the cell structure not only increased but the length of the cells also increased. If the selection mechanism hypothesized by Tam is correct, the elongation of these cells which select the frequency of the disturbance would increase the wavelength of the disturbance. Assuming that the wave speed of the disturbance is a constant percentage of the mean velocity of the jet and that the cell length and the wavelength of the disturbance vary

linearly, the increase in the wavelength due to underexpanding the jet would decrease the frequency of the disturbance. The measurements definitely indicate a decrease in the frequency of the group of modes.

It was observed that the strength of the mean cell structure was the only major difference in the mean flow characteristics of the 9.52 and 6.35 mm jets. If one assumes that the strength of the mean cell structure was the determining factor for multimodal or single modal characteristics of the jet, then increasing the strength of the cell structure in the 6.35 mm jet would produce a single modal jet. However, when the cell structure strength of the 6.35 mm jet is increased by underexpanding the jet to values larger than those present in the 9.52 mm perfectly expanded jet only the spread of the modes is decreased slightly. The picture is further clouded by the fact that on humid days, which correspond to days of higher values for P_n/P_o, spectra of the 6.35 mm jet perfectly expanded have been obtained which are single modal. For example, see Figure 14(a). The exact reason for the spectra changing from multimodal to single modal is not understood, but there are indications that the changing humidity has some effect on the spectra. The multimodal spectra in Figure 8(a) was taken on a day when the ratio of pounds of moisture in the air to the pounds of dry air was 0.0142 while for the spectra in Figure 14(a) the ratio was 0.0205. There was also evidence of a slight drift in the dominant mode's frequency from day to day, but it was only on the order of 5%.

It is evident that more measurements need to be made of the spectral components in the jets with some control over the humidity. In this manner the mode switching characteristics of the jet may be better understood. In addition, the non-linear interaction observed in Figure 14(d) when the 6.35 mm jet was artificially excited at St = 0.148 needs to be

investigated more closely. Measurements should be made when the jet is excited at different frequencies to determine if the non-linear interaction occurs for different excitation frequencies other than St = 0.148. This may give some insight to the structure of the multimodal jet and how the disturbances present in the jet interact.

In conjunction with a more extensive multimodal investigation, more measurements on the growth rates of individual spectra components are needed. The growth rates presented in the thesis were specified as being preliminary since the fluctuation measurements were made at the radial position of maximum fluctuation for the entire spectrum of frequencies present in the jet. Therefore, the spatial distribution (radial) of the fluctuations of a given spectral component needs to be determined and growth rates based upon the maximum fluctuation at each x/D location should be made. It may be desirable to perform these measurements with zero percent humidity in order to diminish the tendency of the naturally occuring spectral components to vary in amplitude from day to day.

This study is part of an overall research of the aerodynamic noise of a supersonic jet. In addition to stability measurements, microphone measurements in the acoustic field of the jet have been made by Troutt (21).

Figure 19 consists of microphone spectra for the three jets operating in the perfectly expanded condition. These spectra were made by Troutt (21) in the same flow facility as the present measurements. The Strouhal numbers of the major acoustic modes in each jet correspond to approximately the same Strouhal number of the major modes in the hot-wire spectra of Figure 8. This indicates that flow disturbances in the jet are radiating sound at the same Strouhal number as the disturbances.

For the 6.35 mm and 15.9 mm jets the microphone spectra do not contain all of the major modes present in the hot-wire spectra. This indicates that not all of the modes are interacting with the surrounding air in the same manner since apparently some of the modes are more efficient acoustic emitters than others. The microphone spectra of the 9.35 mm jet contains only the single mode of Strouhal number 0.17 as was the case with the hot-wire spectra for the same nozzle.

Acoustic phase measurements similar to the hot-wire phase measurements were performed in the 6.35 mm jet by Troutt (21). He found that the acoustic wavelength in the x direction is approximately the same as the instability disturbance wavelength. The acoustic wavelength (λ_x/D) is 3.25 ± 0.30 compared to an instability wavelength of 3.20 ± 0.30. Troutt measured the angle θ at which the acoustic wave fronts propagate away from the jet and determined the angle to be $57.5° \pm 4°$. This angle is in agreement with the Mach wave concept in that a Mach angle computed from the wave speed C yields a Mach angle of $60.2° \pm 2°$.

These measurements show that the instability waves present in the jet are generating a major portion of the sound radiated by a low Reynolds number supersonic jet. Thus the motivation for better understanding the instabilities is clearly established.

BIBLIOGRAPHY

(1) Lighthill, M. J. "On Sound Generated Aerodynamically, I General Theory." Proc. Roy. Soc., A211 (1952), pp. 546-587.

(2) Lighthill, M. J. "On Sound Generated Aerodynamically, II Turbulence as a Source of Sound." Proc. Roy. Soc., A222 (1954), pp. 1-32.

(3) Ffowcs Williams, J. E. "The Noise From Turbulence Convected at High Speed." Phil. Trans. Roy. Soc., A255 (1963), p. 459.

(4) Crow, S. C., and F. H. Champagne. "Orderly Structure in Jet Turbulence." J. Fluid Mech., Vol. 48 (1971), pp. 547-591.

(5) Bishop, K. A., J. E. Ffowcs Williams, and W. Smith. "On the Noise Sources of the Unsuppressed High-Speed Jet." J. Fluid Mech., Vol. 50 (1971), pp. 21-31.

(6) Phillips, O. M. "On the Generation of Sound by Supersonic Turbulent Shear Layer." J. Fluid Mech., Vol. 9 (1960), pp. 1-28.

(7) Tam, C. K. W. "On the Noise of a Nearly Ideally Expanded Supersonic Jet." J. Fluid Mech., Vol. 51 (1972), pp. 69-95.

(8) Tam, C. K. W. "Directional Acoustic Radiation From a Supersonic Jet Generated by Shear Layer Instabilities." J. Fluid Mech., Vol. 46 (1971), pp. 757-768.

(9) Tam, C. K. W. "Supersonic Jet Noise Generated by Large Scale Disturbances." AIAA Paper 73-992, 1973.

(10) Sedel'nikov, T. Kh. "The Frequency Spectrum of the Noise of a Supersonic Jet." Phy. of Aero. Noise. Moscow: Nauka Press, (Translated NASA TTF-538, 1969, 71-75).

(11) Chan, Y. Y., and R. Westley. "Directional Acoustic Radiation Generated by Spatial Jet Instability." CASI Trans., Vol. 6 (1973), pp. 36-41.

(12) Matthews, M. L. "An Experimental Investigation of Viscous Effects on Static and Impact Pressure Probes in Hypersonic Flow." Pasedena, California: GALCIT, Hypersonic Research Project, Memo 44, 1958.

(13) Behrens, W. "Viscous Interaction Effect on a Static Pressure Probe at M = 6." AIAA J., Vol. 1 (1963), pp. 2364-2366.

(14) Morkovin, M. W. "Fluctuations and Hot-Wire Anemometry in Compressible Flows." AGARDograph No. 24, 1956.

(15) Rose, W. C. "The Behavior of a Compressible Turbulent Boundary Layer in a Shock Wave Induced Adverse Pressure Gradient." (Ph.D dissertation, University of Washington, 1972, available as NASA TN D-7092.)

(16) Behrens, W. "Flow Field and Stability of the Far Wake Behind Cylinders at Hypersonic Speeds." (Ph.D. dissertation, California Institute of Technology, Pasedena, California, 1966.)

(17) Behrens, W. "Far Wake Behind Cylinders at Hypersonic Speeds: II Stability." AIAA J., Vol. 6 (1968), pp. 225-232.

(18) Kendall, J. M. Jr. "Supersonic Boundary Layer Stability Measurements." Proc. of the Boundary Layer Trans. Study Group, Meeting II, Aerospace Rept. TR-0158, (S3816-63)-1, 1967.

(19) Miksad, R. W. "Experiments on Non-Linear Interactions in the Transition of a Free Shear Layer." J. Fluid Mech., Vol. 59 (1973), pp. 1-21.

(20) Sato, H. "An Experimental Study of Non-Linear Interaction of Velocity Fluctuations in the Transition Region of a Two-Dimensional Wake." J. Fluid Mech., Vol. 44 (1970), pp 741-765.

(21) Troutt, T. R. "Noise Measurements of a Low Reynolds Number Supersonic Jet." (Unpub. M.S. thesis, Oklahoma State University, 1974.)

APPENDIX A

FIGURES

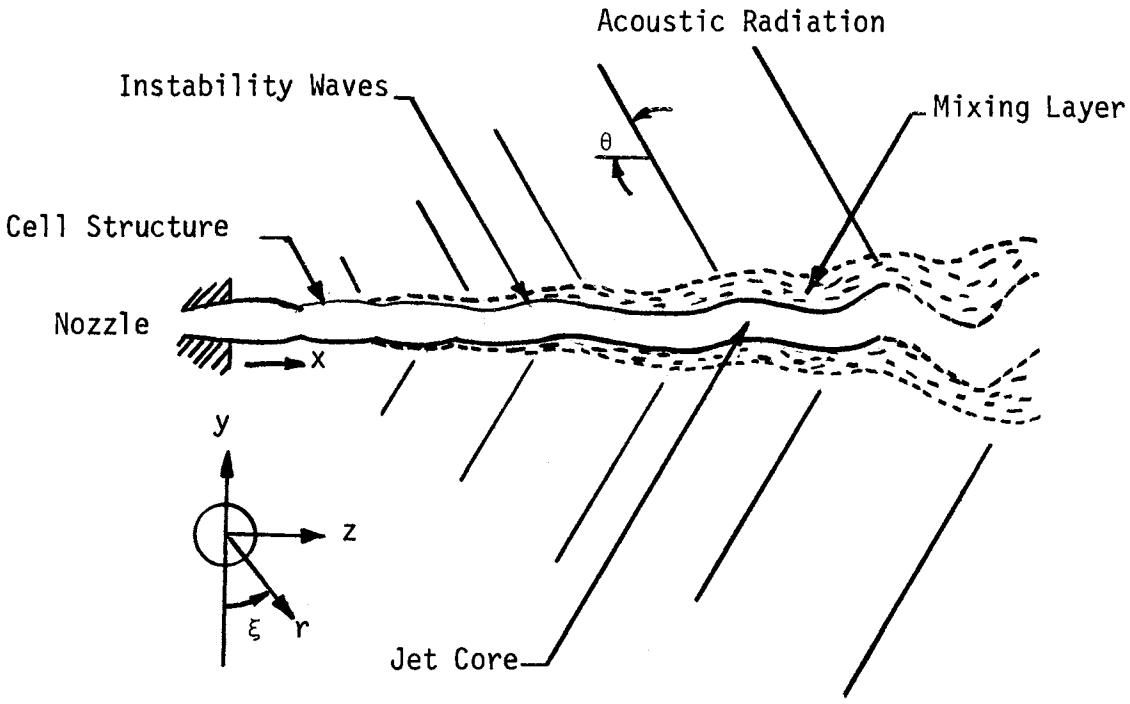

Figure 1. General Features of the Supersonic Jet and its Acoustic Radiation

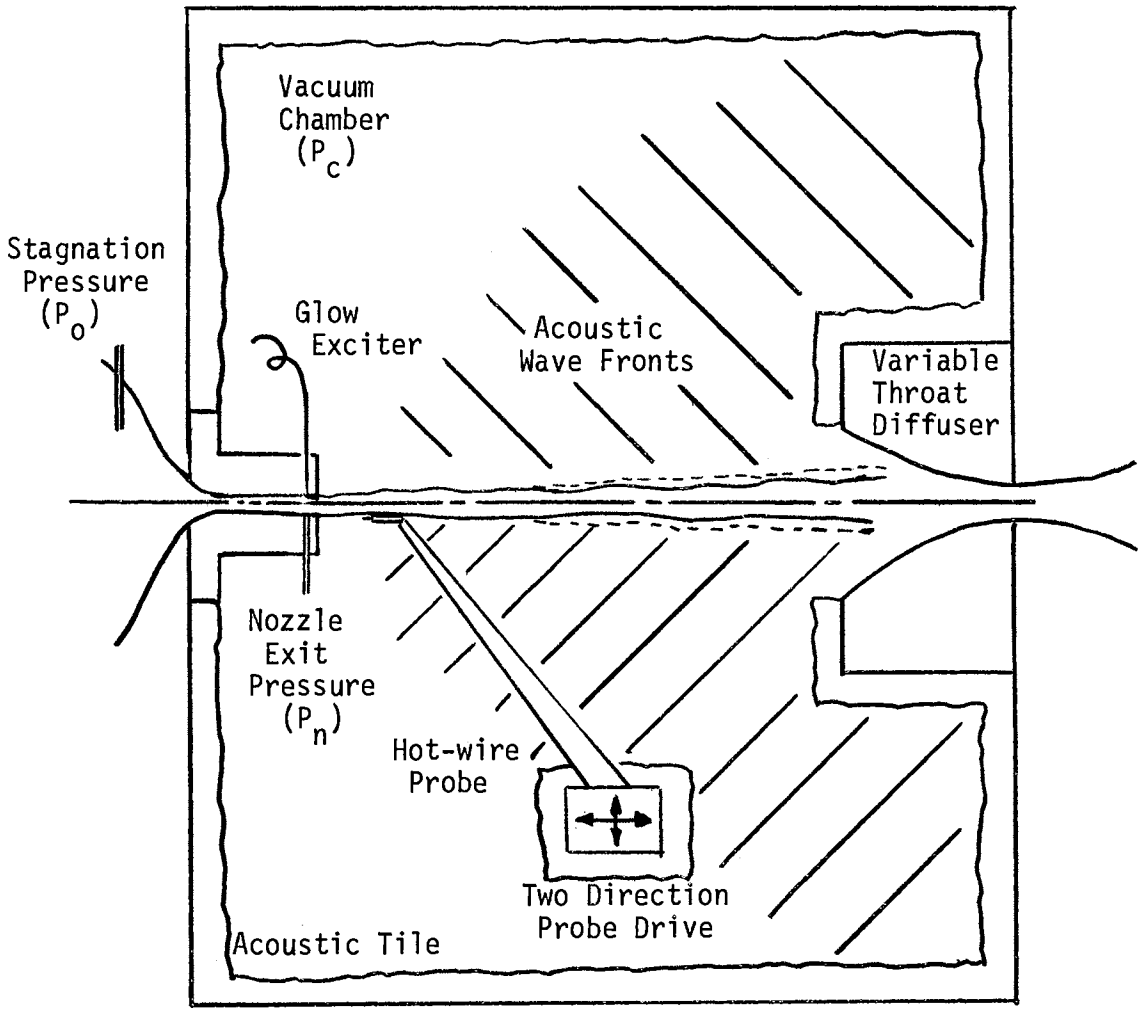

Figure 2. Schematic of the Supersonic Jet Test Facility

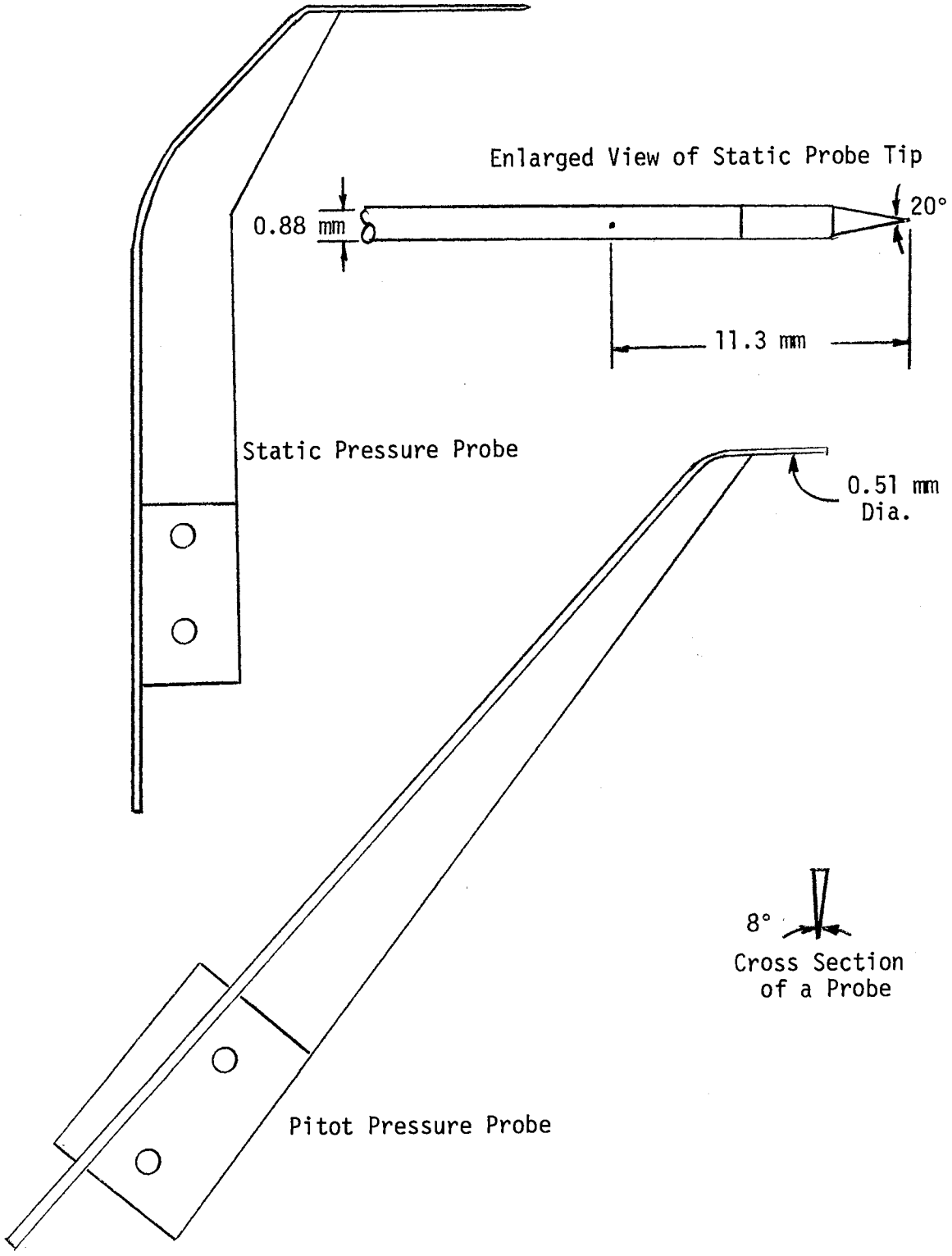

Figure 3. Static Pressure and Pitot Pressure Probes Drawn Full Scale

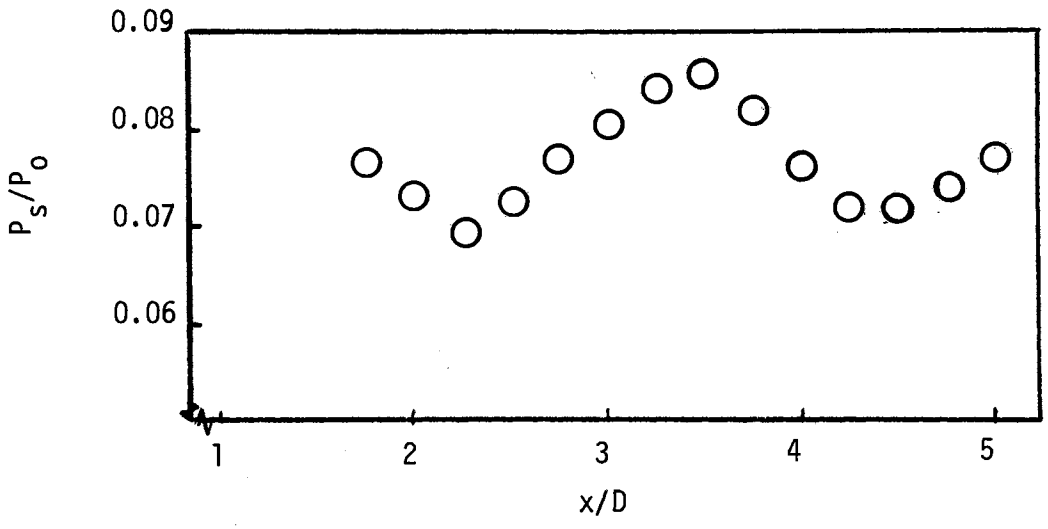

(a) D = 6.35 mm, P_n/P_c = 1.01, Re = 12,100

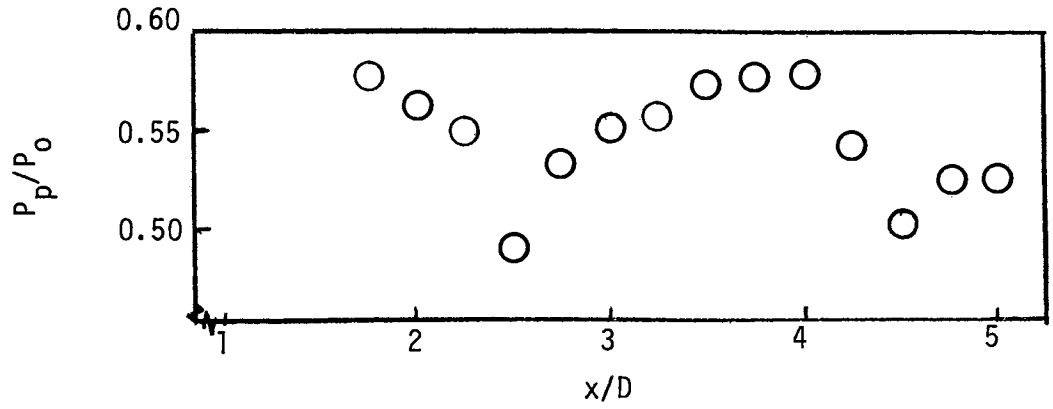

(b) D = 6.35 mm, P_n/P_c = 1.01, Re = 12,100

Figure 4. Axial Distribution of Centerline Static Pressure and Pitot Pressure Measurements

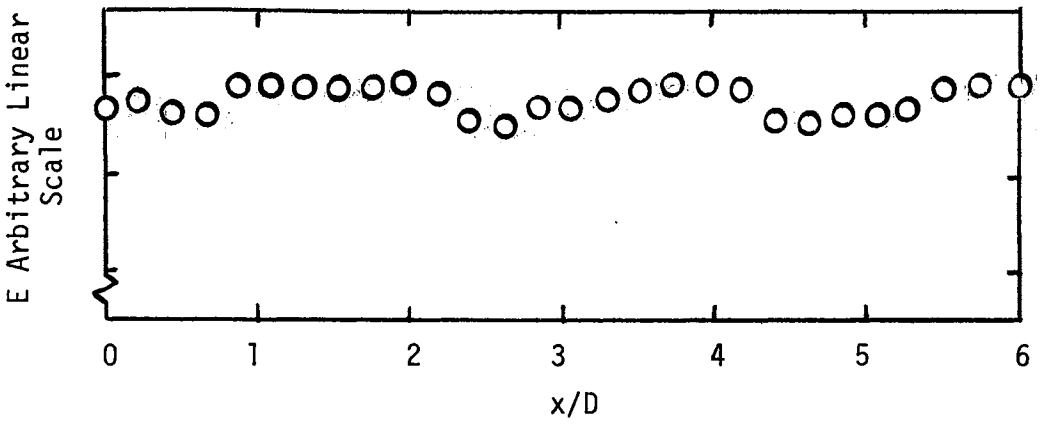

(a) D = 6.35 mm, P_n/P_c = 1.01, Re = 12,800

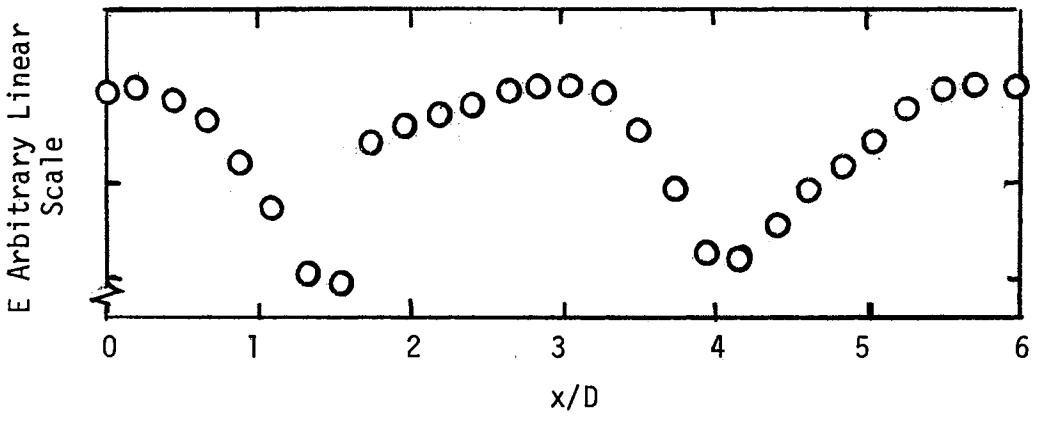

(b) D = 6.35 mm, P_n/P_c = 1.5, Re = 12,700

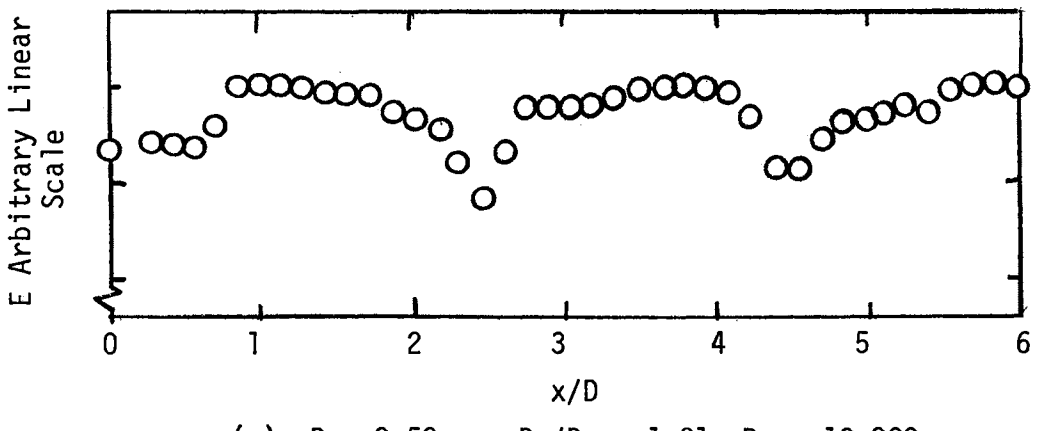

(c) D = 9.52 mm, P_n/P_c = 1.01, Re = 19,900

Figure 5. Axial Distribution of Centerline Mean Hot-Wire Voltage Showing Mean Flow Variations

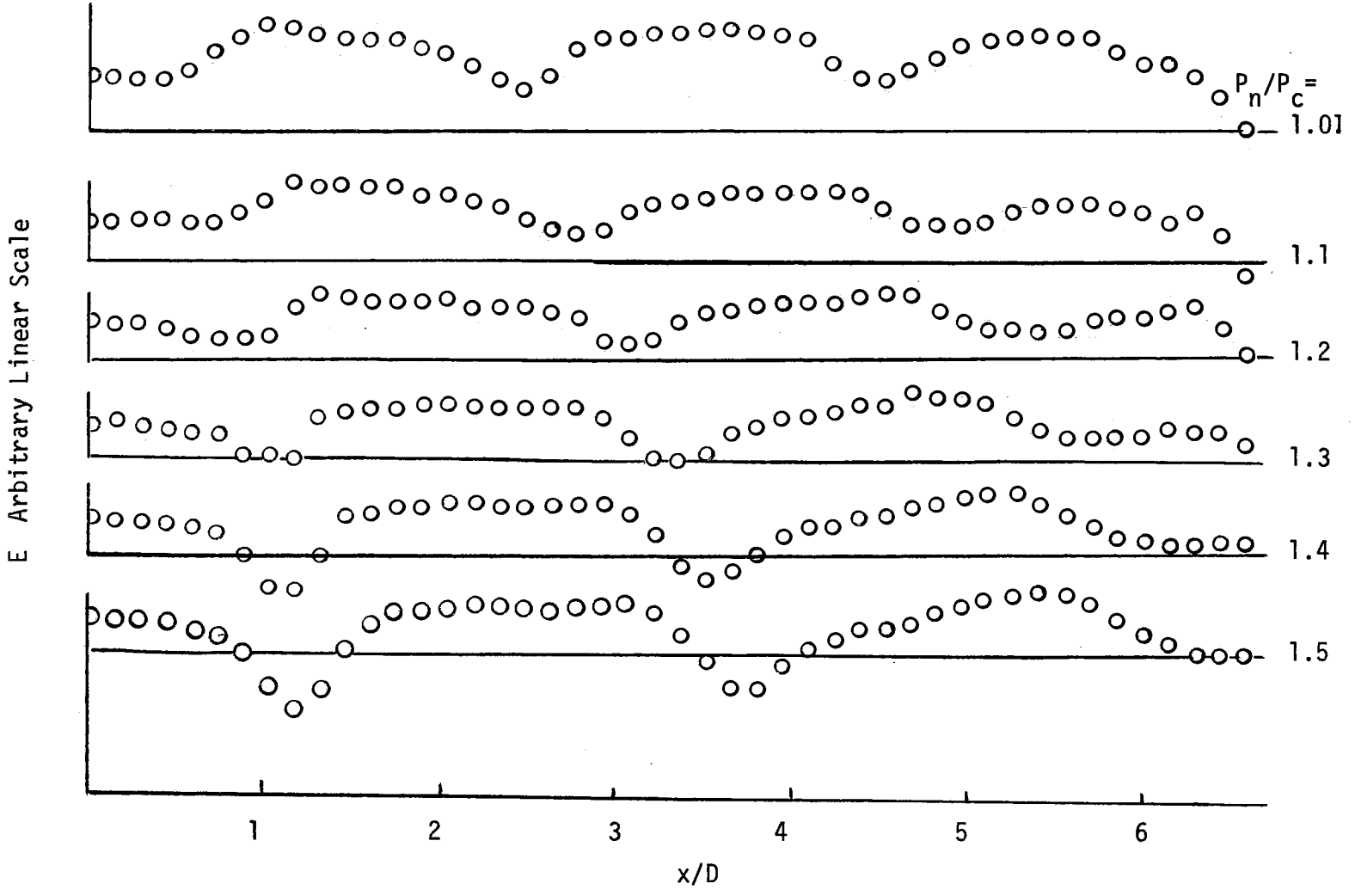

Figure 6. Mean Hot-Wire Voltage at Various x/D Locations and Ratios of P_n/P_c

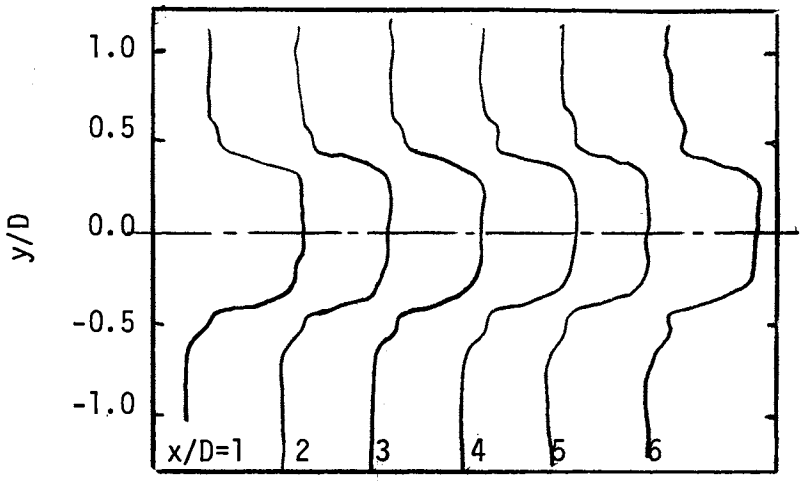

(a) D = 6.35 mm, P_n/P_c = 1.01,
Re = 12,900

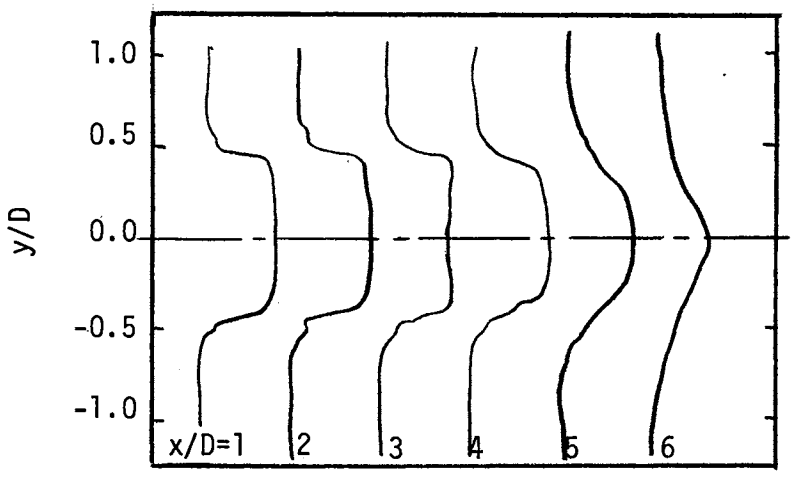

(b) D = 9.52 mm, P_n/P_c = 1.01
Re = 22,800

Figure 7. Profiles of Mean Hot-Wire Voltage at Various Downstream Locations

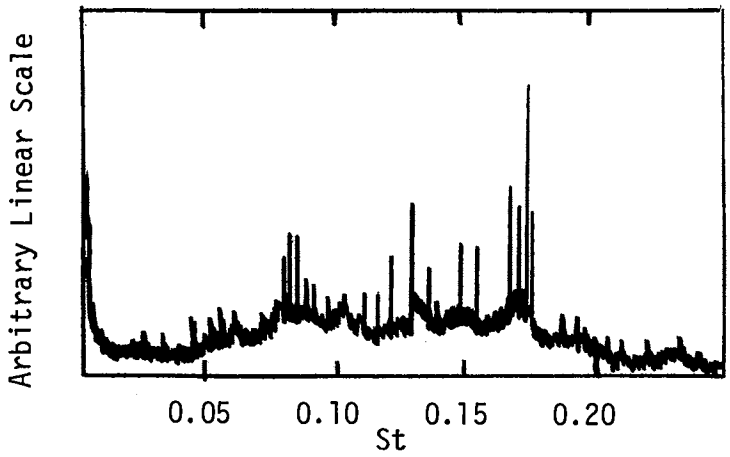

(a) D = 6.35 mm, Re = 13,000, U/d = 105,000/sec.

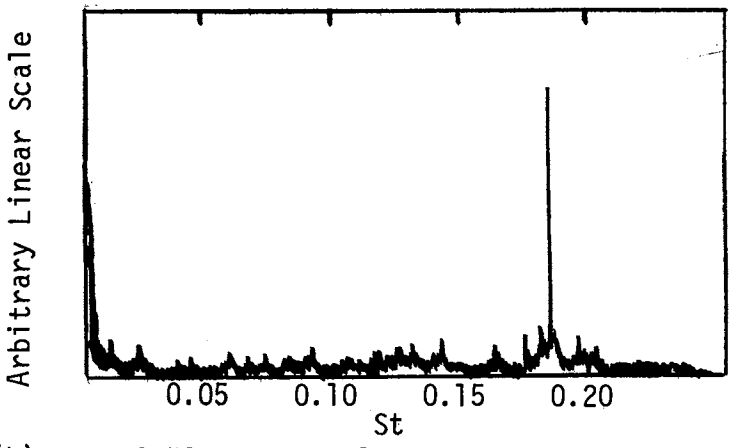

(b) D = 9.52 mm, Re = 14,600, U/d = 67,800/sec.

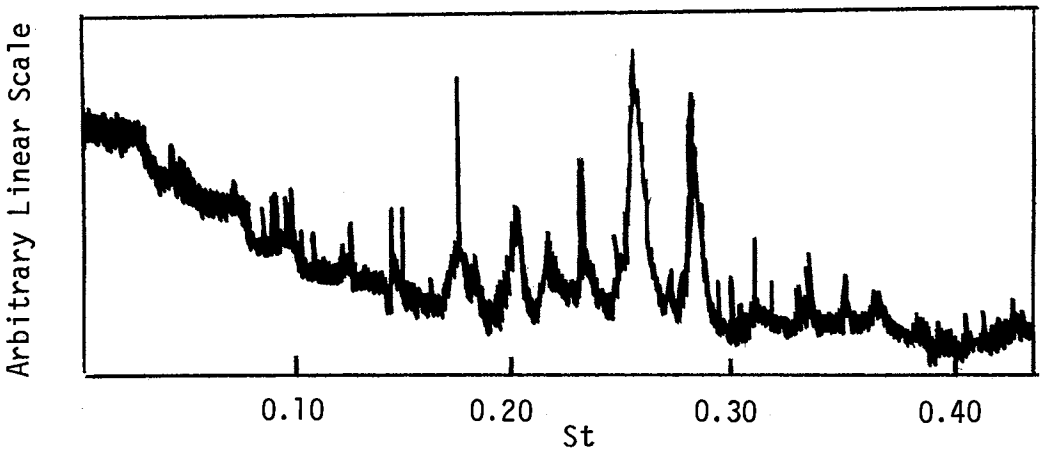

(c) D = 15.9 mm, Re = 15,200, U/d = 38,700/sec.

Figure 8. Hot-Wire Voltage Fluctuation Frequency Spectra for Perfectly Expanded Jets

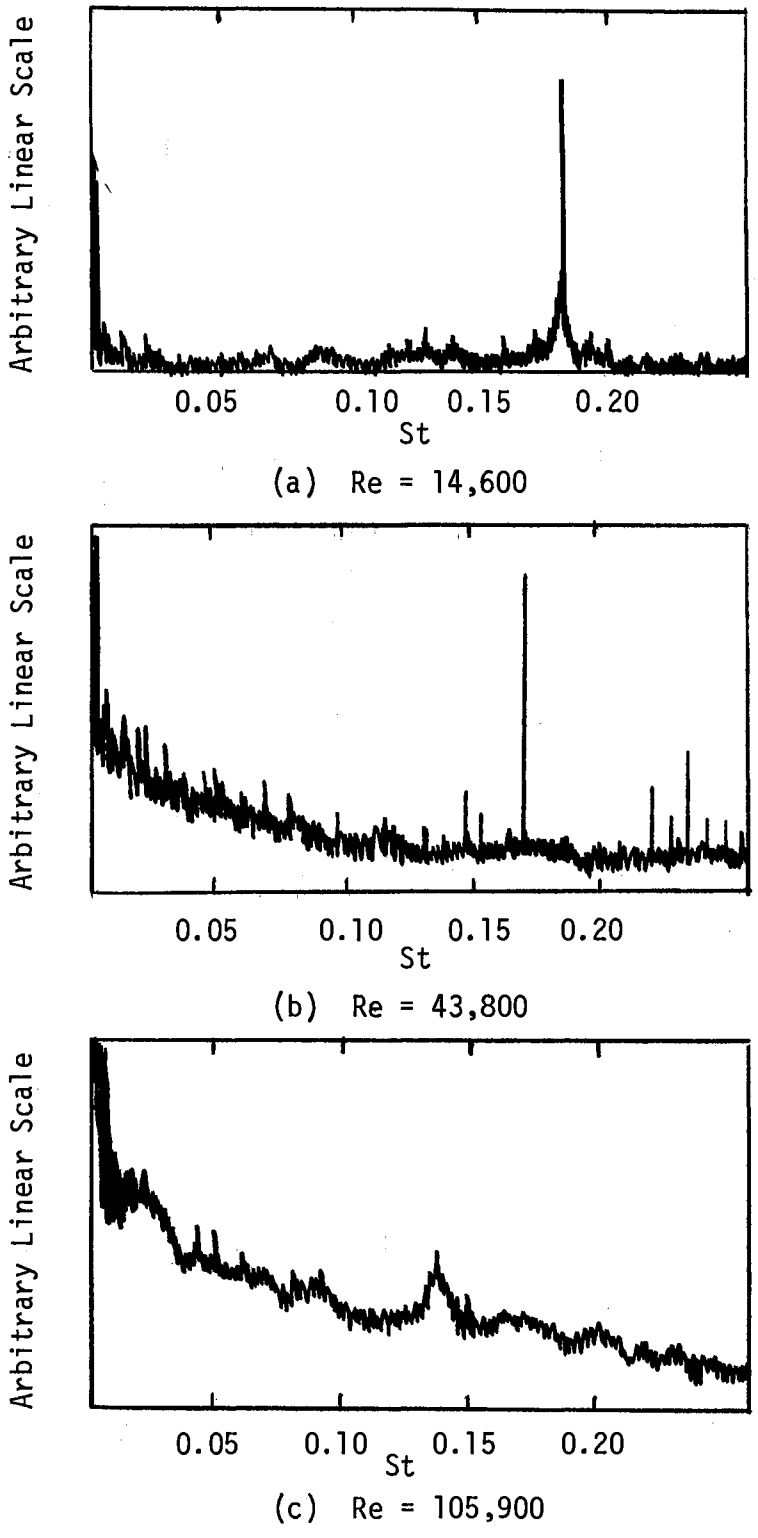

Figure 9. Effect of Increasing the Reynolds Number on Hot-Wire Voltage Fluctuation Frequency Spectra, D = 9.52 mm.

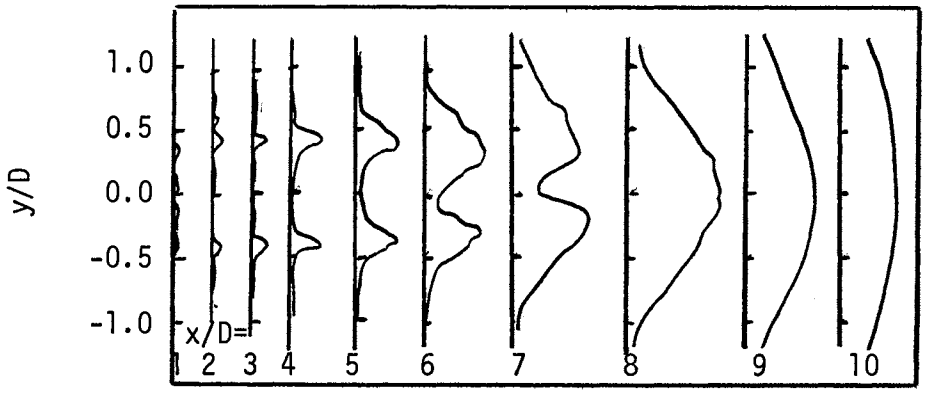

e'_{rms} Arbitrary Linear Scale

(a) D = 9.52 mm, P_n/P_c = 1.01, Re = 14,700

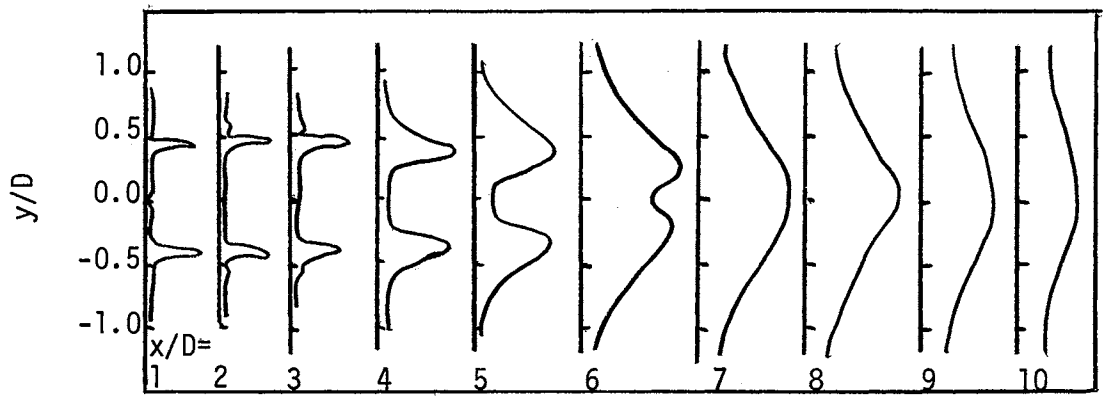

e'_{rms} Arbitrary Linear Scale

(b) D = 9.52 mm, P_n/P_c = 1.01, Re = 44,100

Figure 10. Profiles of Root Mean Square Hot-Wire Voltage Fluctuations at Various Downstream Locations

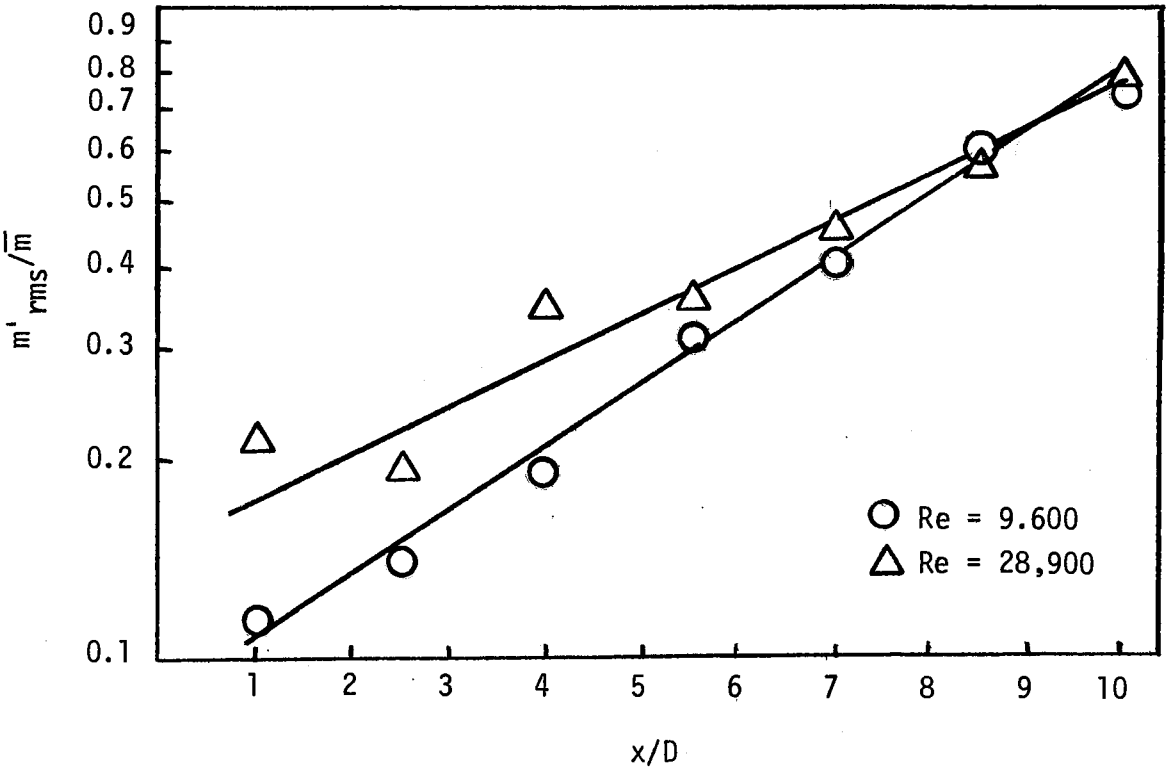

Figure 11. Axial Distribution of Peak Hot-Wire Voltage Fluctuations

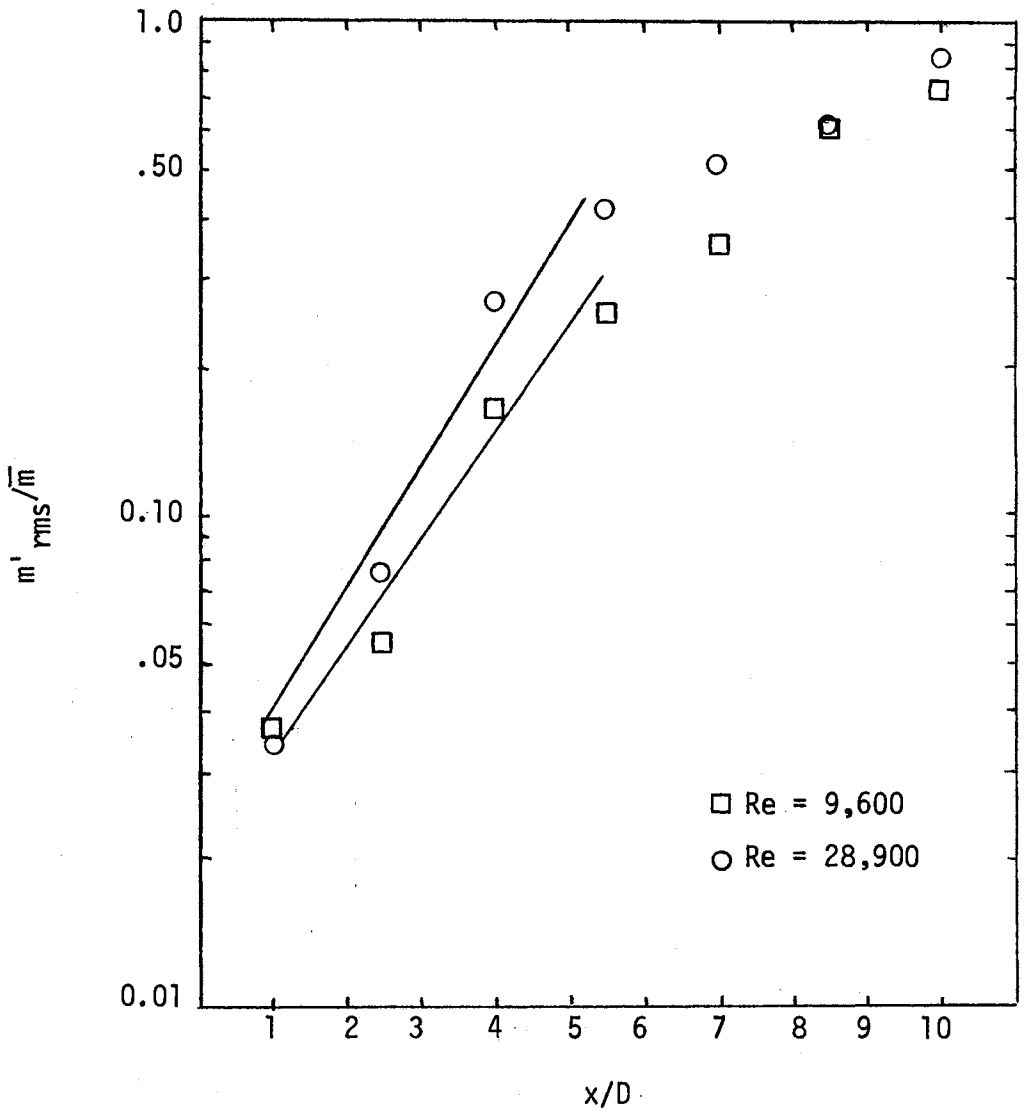

Figure 12. Axial Distribution of Peak Hot-Wire Voltage Fluctuations, High Pass Filter is 1000 Hz

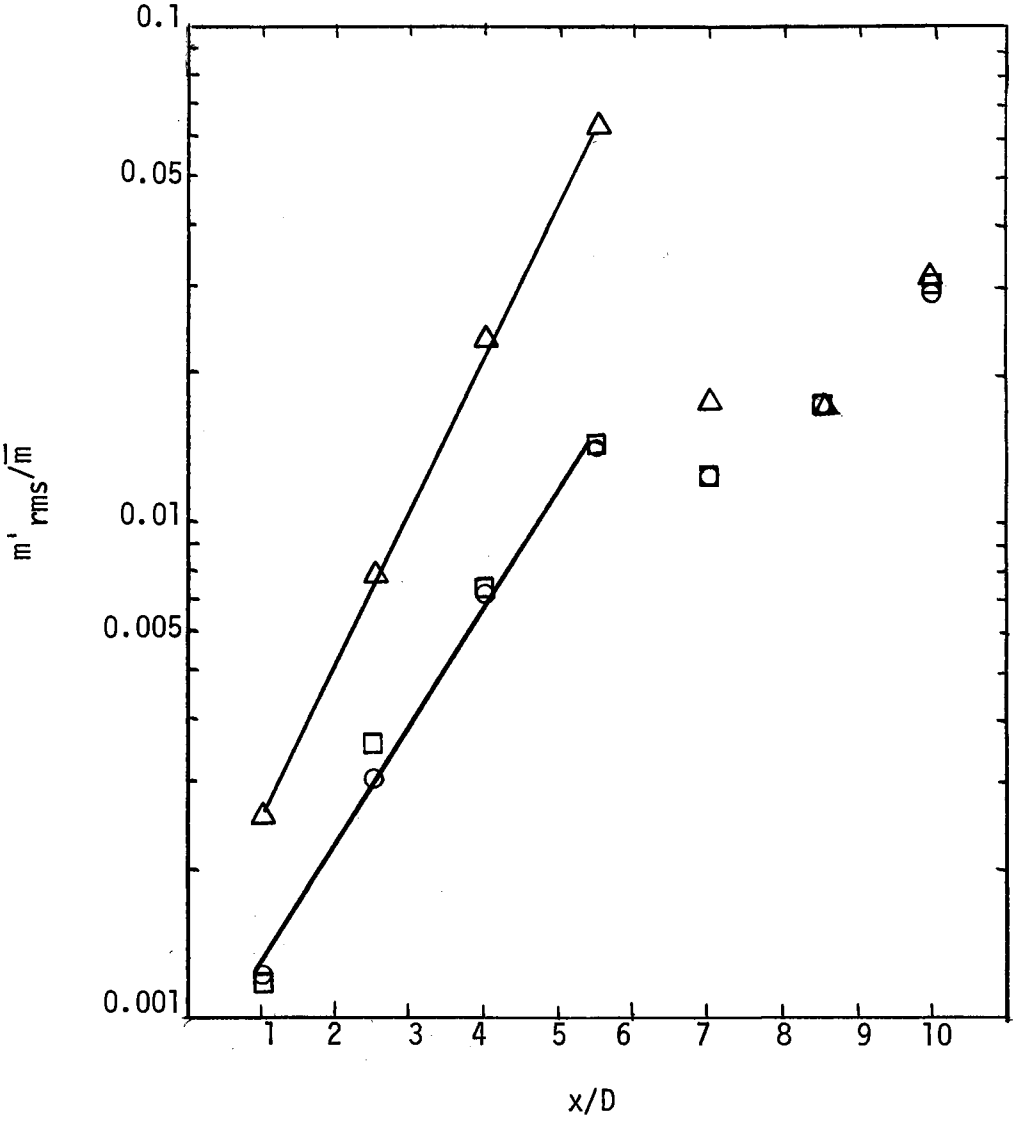

Figure 13. Axial Distribution of Peak Hot-Wire Voltage Fluctuations for a 100 Hz Wide Band Centered about △ St = 0.148, □ St = 0.176, ○ St = 0.185, Re = 28,900

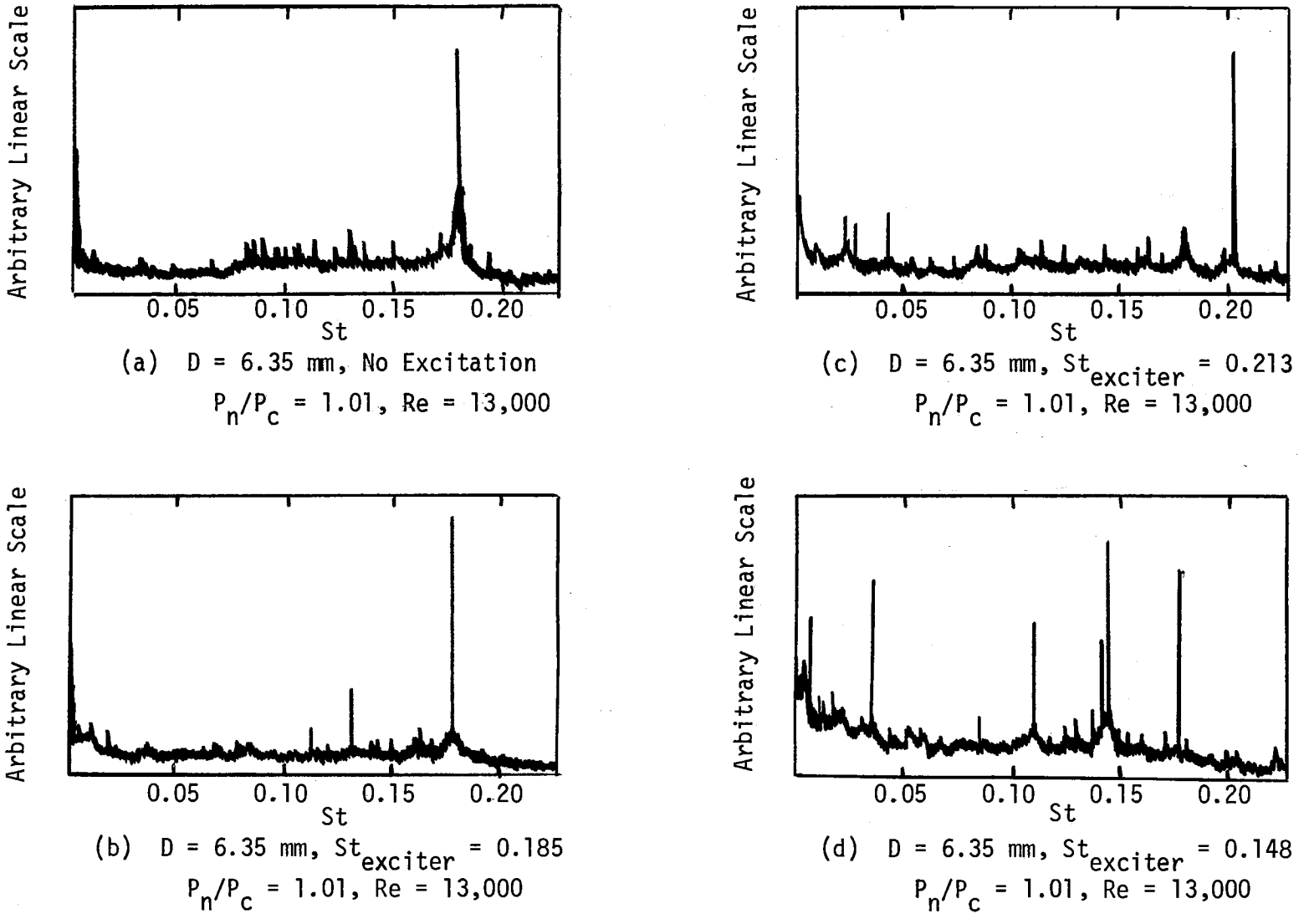

Figure 14. Effect of Excitation on the Hot-Wire Frequency Spectrum

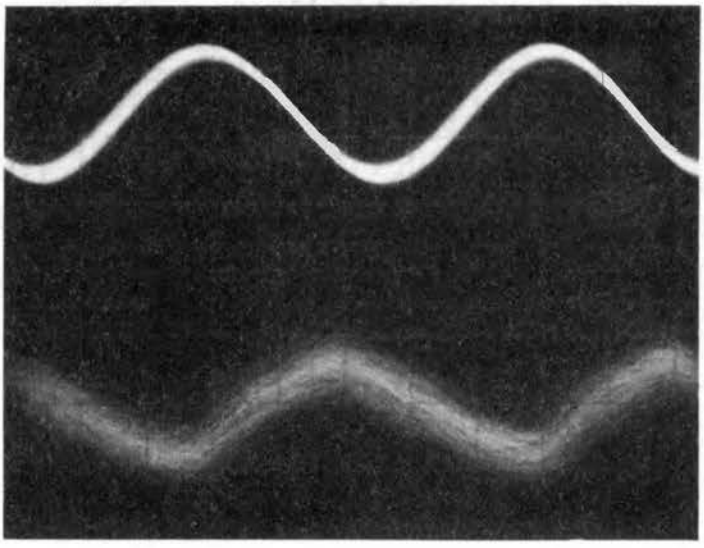

Figure 15. Oscilloscope Trace of Exciter (Upper Trace) and Instaneous Hot-Wire Signal (Lower Trace) Showing a Typcial Phase Lock Situation; D = 6.35 mm, $(x/D)_{probe}$ = 5, Sweep Rate = 10μ sec/cm

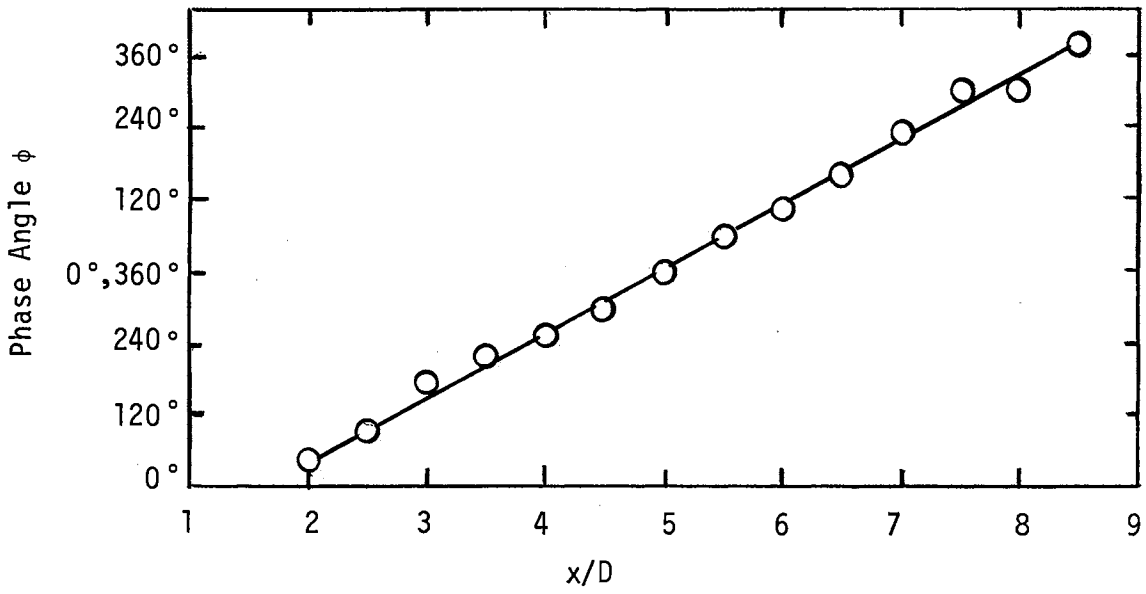

Figure 16. Axial Distribution of Hot-Wire Phase;
D = 9.52 mm, Re = 14,700, St = 0.17

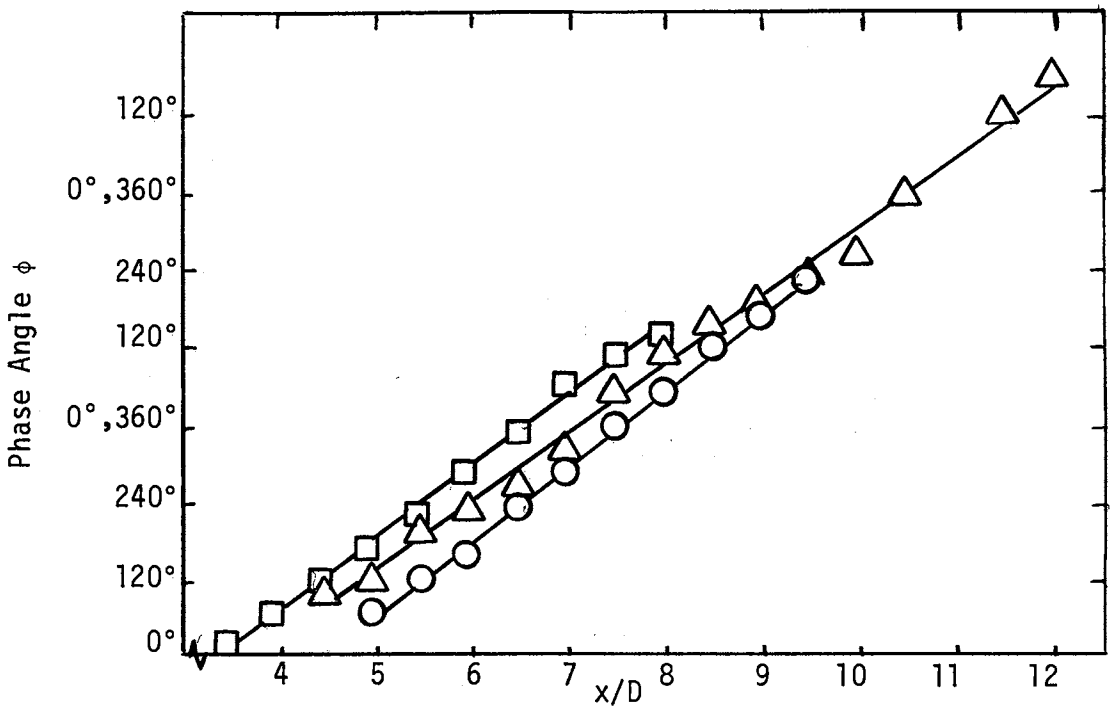

(a) □ $\lambda_x/D = 3.18 \pm 0.18$, △ $\lambda_x/D = 3.34 \pm 0.16$, ○ $\lambda_x/D = 3.03 \pm 0.12$, St = 0.185

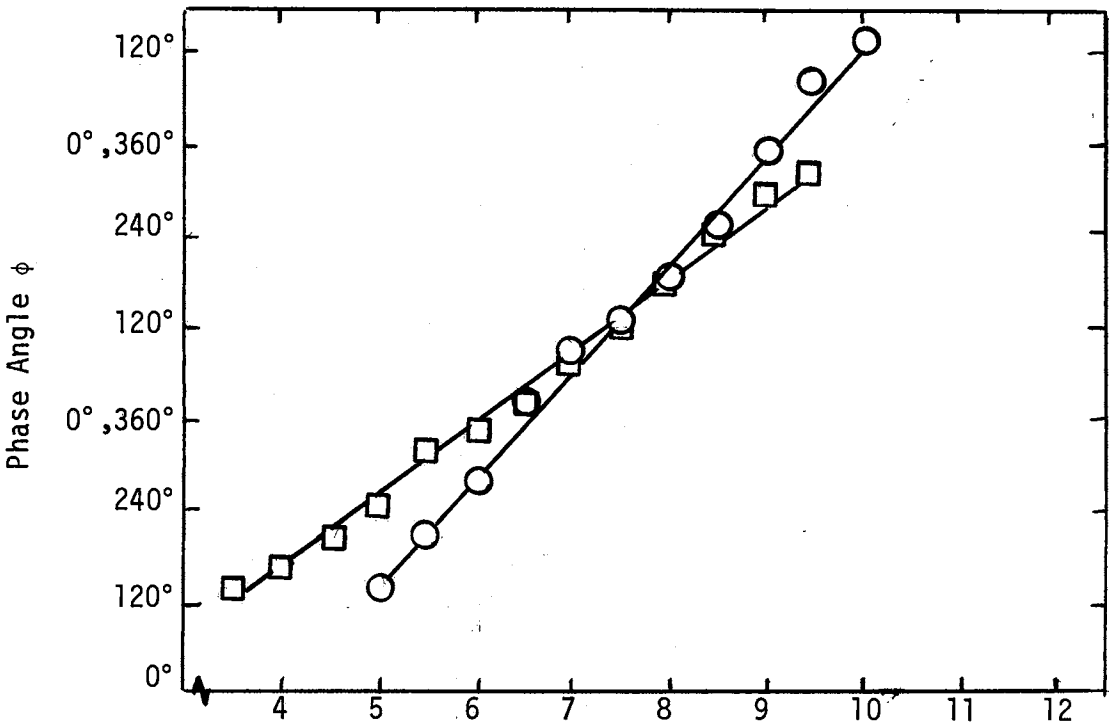

(b) ○ $\lambda_x/D = 2.57 \pm 0.18$, St = 0.213, □ $\lambda_x/D = 3.88 \pm 0.30$, St = 0.148

Figure 17. Axial Distribution of Hot-Wire Relative Phase; D = 6.35mm, Re = 20,000

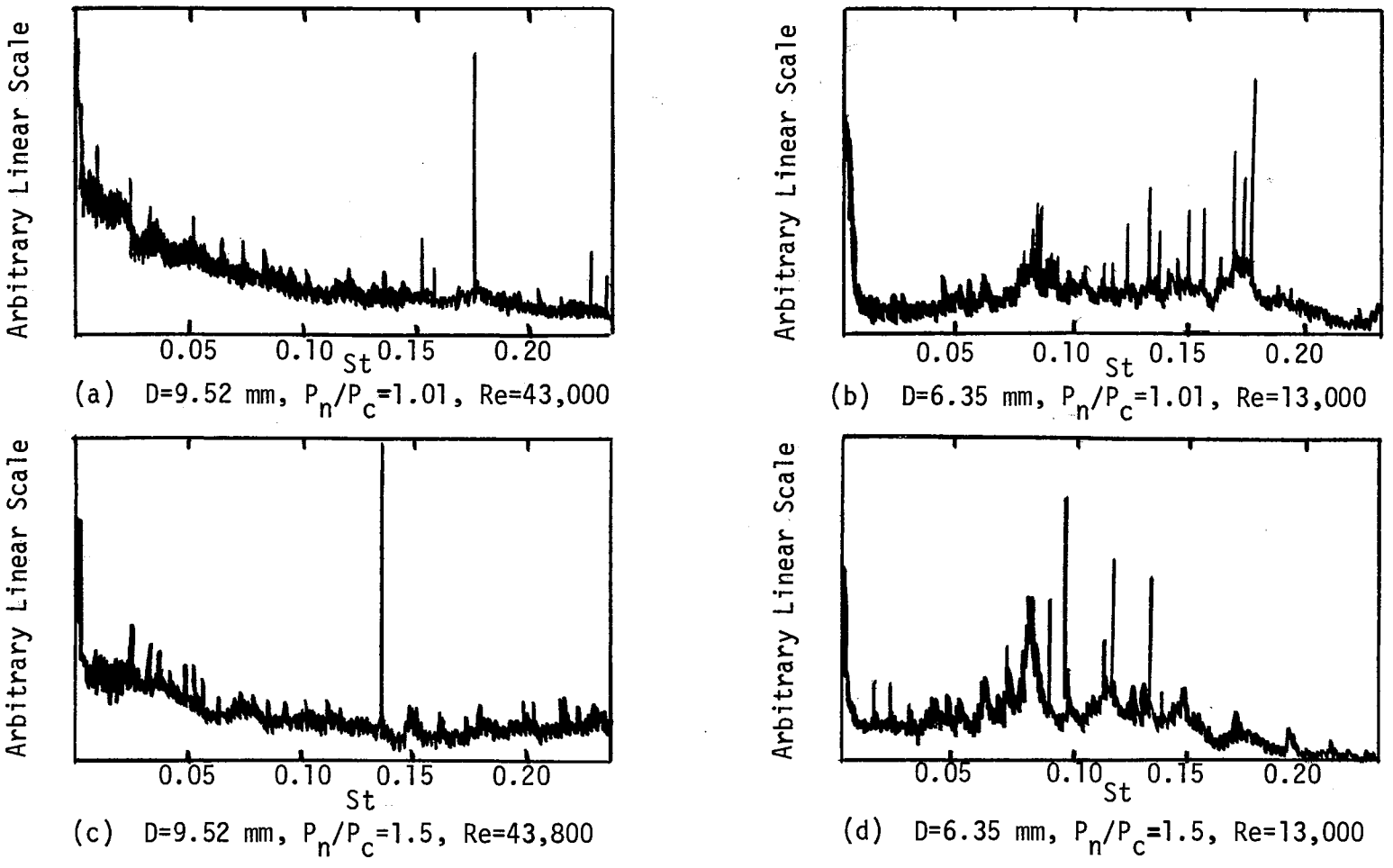

Figure 18. Effect of Underexpansion on the Hot-Wire Voltage Fluctuation Frequency Spectra

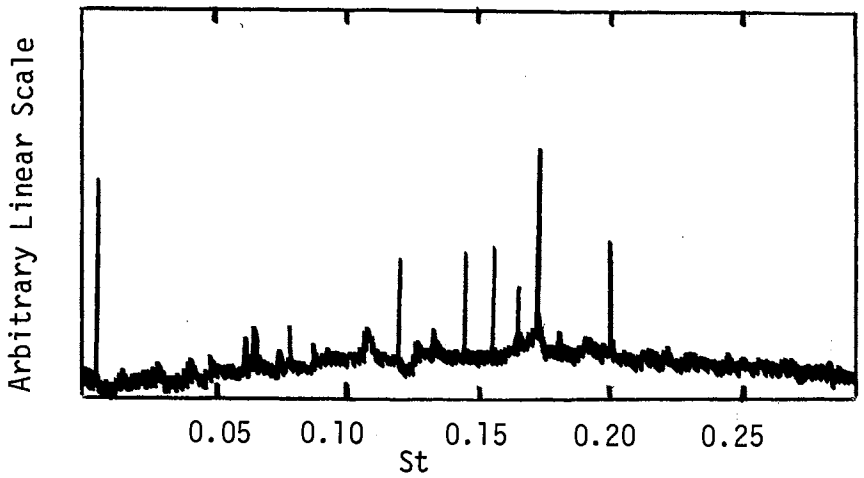

(a) D = 6.35 mm, Re = 12,600

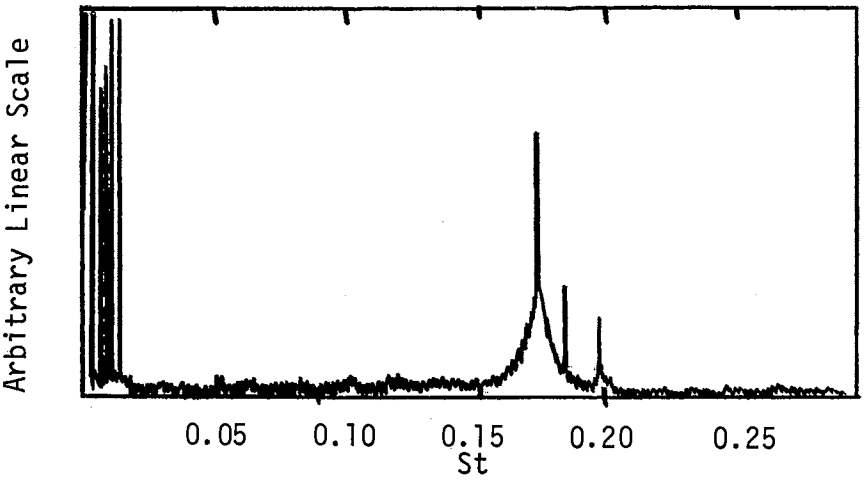

(b) D = 9.52 mm, Re = 11,000

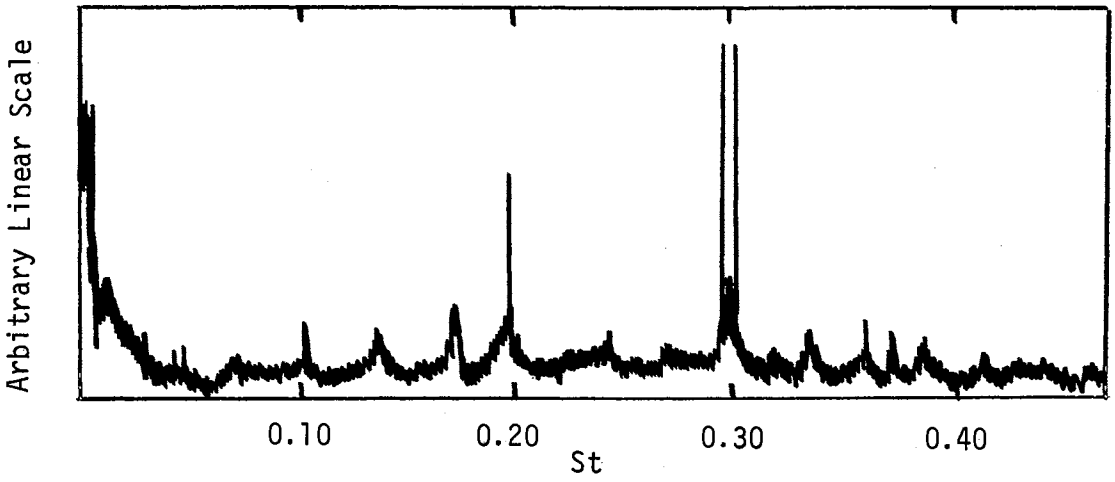

(c) D = 15.9 mm, Re = 16,300

Figure 19. Microphone Frequency Spectra in the Acoustic Field of Perfectly Expanded Jets

APPENDIX B

TABLES

TABLE I

COMPARISON OF MEASURED TO PREDICTED GROWTH RATES FOR THE 6.35 mm JET, M = 2.2

St	Growth Rate $-K_I d$	
	Measured	Tam Prediction
0.148	0.58	0.64
0.176	0.44	0.76
0.185	0.44	0.82

TABLE II

COMPARISON OF MEASURED VALUES OF k_R AND St TO VALUES PREDICTED BY TAM

D (mm)	Measured		Predicted by Tam	
	St	$k_R d$	$k_R d$	St (dominant)
6.35	0.148	1.34	1.10	
6.35	0.185	1.60	1.42	0.193 ($k_R d$=1.47)
6.35	0.213	1.99	1.66	
9.52	0.170	1.65	1.28	0.198 ($k_R d$=1.50)

VITA

Gerald Lee Morrison

Candidate for the Degree of

Master of Science

Thesis: STABILITY MEASUREMENTS IN A LOW REYNOLDS NUMBER SUPERSONIC JET

Major Field: Mechanical Engineering

Biographical:

Personal Data: Born in Bartlesville, Oklahoma, October, 1951, the son of Mr. and Mrs. E. R. Morrison.

Education: Graduated from Sooner High School in Bartlesville, Oklahoma in May, 1969; received the Bachelor of Science Mechanical Engineering at Oklahoma State University in May, 1973; completed requirements for the Master of Science degree at Oklahoma State University in May, 1974.

Honors: Phi Kappa Phi, Pi Tau Sigma, Sigma Tau, Tau Beta Pi, and Gulf Oil Fellowship.

Professional Societies: American Institute of Aeronautics and Astronautics.